Crack Turning and Arrest Mechanisms for Integral Structure

Final Report

NASA Contract NAG-1-2013

Richard Pettit
Anthony Ingraffea

Cornell University
December 31, 1999

TABLE OF CONTENTS

1.0 BACKGROUND

This project is part of a larger, ongoing research effort at Cornell University to develop theory and simulation methods suitable for predicting crack turning and arrest in integral aircraft structures. In addition to the documents included with this report, documentation of work completed throughout the entire project, including work accomplished after the period of performance for the present program, will be compiled in the form of a doctoral dissertation planned for completion by August 2000.

2.0 ACCOMPLISHMENTS

A key accomplishment of the present program was the development and implementation of the second-order linear-elastic crack turning theory with fracture toughness orthotropy into the FRANC2D fracture simulation code. An early version of the code has already found use in analyses performed under the Integral Airframe Structure (IAS) Program (Contract NAS1- 20014, Task 34, ending November, 1998). Correlation of crack path predictions with observed trajectories in test specimens for a variety of test conditions was much better than would be expected of any other known theory. Since that time, the code has been further improved to reflect new T-stress calculation techniques described in Attachment #1, among other improvements.

In a collaborative effort, the code driving the second-order orthotropic crack turning theory was ported to the shell version of FRANC3D to study crack turning and flapping of narrow body fuselage structure under the aging aircraft program.

A theoretical estimate of the characteristic length, r_c, associated with crack turning, has been developed based on the concept of plastic instability. This parameter is necessary for application of the 2nd order theory. This work is also described in Attachment #1.

With regard to the turning criterion, it has been found that a very similar angle prediction to the 2nd order theory max stress theory can be obtained based on elastic CTOD theory. The solution is sensitive to the T-stress (in the same manner as the maximum tangential stress theory), and to the length of the crack extension (which is roughly equivalent to r_c). A description of this finding and a proposed extension to the elastic plastic case is described in Attachment #2.

Test plans and specimens were also prepared under the present program for testing under a later segment of the overall effort, and an interpolating function for 3D fracture toughness orthotropy was also developed to support future development of a 3D crack turning simulation capability (applicable to thick structures).

3.0 ATTACHMENTS

Evaluation of the Characteristic Length and T-stress for 2nd Order Crack Turning Problems

Richard G. Pettit
Anthony R. Ingraffea

Cornell Fracture Group

Attachment #1 to Final Report
NASA Contract NAG-1-2013

December, 1999

ABSTRACT

In the course of several years of research efforts to predict crack turning and flapping in aircraft fuselage structures and other problems related to crack turning, the 2nd order maximum tangential stress theory has been identified as the theory most capable of predicting the observed test results. This theory requires knowledge of a material specific characteristic length, and also a computation of the stress intensity factors and the T-stress, or second order term in the asymptotic stress field in the vicinity of the crack tip.

A characteristic length, r_c, is proposed for ductile materials pertaining to the onset of plastic instability, as opposed to the void spacing theories espoused by previous investigators. For the plane stress case, an approximate estimate of r_c is obtained from the asymptotic field for strain hardening materials given by Hutchinson, Rice and Rosengren (HRR).

A previous study using of high order finite element methods to calculate T-stresses by contour integrals resulted in extremely high accuracy values obtained for selected test specimen geometries, and a theoretical error estimation parameter was defined. In the present study, it is shown that a large portion of the error in finite element computations of both K and T are systematic, and can be corrected after the initial solution if the finite element implementation utilizes a similar crack tip discretization scheme for all problems. This scheme is applied for two-dimensional problems to a both a p-version finite element code, showing that sufficiently accurate values of both K_I and T can be obtained with fairly low order elements if correction is used. T-stress correction coefficients are also developed for the singular crack tip rosette utilized in the adaptive mesh finite element code FRANC2D, and shown to reduce the error in the computed T-stress significantly. Stress intensity factor correction was not attempted for FRANC2D because it employs a highly accurate quarter-point scheme to obtain stress intensity factors.

TABLE OF CONTENTS

1.0 INTRODUCTION

Crack turning has been recognized as a potentially important crack arrest mechanism for pressurized aircraft fuselage structure, and for longitudinal cracks can result in turning and flapping as shown in Figure 1 as reported by Maclin [1]. This behavior contains the damage, vents the pressure in a controlled manner, and results in obvious damage which can be subsequently repaired. Flapping was observed to occur reliably enough during tests of thin skinned, relatively narrow-body fuselages that it was utilized as a fail-safe criterion on the 707, 727, and 737 fuselages for regions excluding the joint areas. Similar phenomena have been observed in unstiffened cylinders by Swift [2], who also reported turning and cracking in an experimental fuselage with adhesively bonded stiffeners [3], and Pettit [4], who observed crack turning and arrest in integrally stiffened fuselage structure with transverse cracks.

These behaviors were observed in tests, but were never successfully modeled until recently. Turning and flapping was observed in narrow-body aircraft, but not wide-body aircraft like the 747 aircraft, and no one really understood why. Also, it was found that aging aircraft develop multi-site damage, which can potentially alter the crack turning and flapping performance [5]. The need for an accurate crack trajectory modeling capability was evident.

In the last decade, a sequence of authors have studied the fuselage flapping phenomenon, including Kosai et al [6], Miller et al [7], Potyondy et al [8], Knops [9], and Chen [10]. Beginning with Potyondy, an adaptive mesh finite element routine was used similar to that proposed by Wawrzynek and Ingraffea [11] but extended to three dimensional shell problems, which allows the trajectory of the crack to develop naturally in accordance with a user-selected crack turning theory. Potyondy used the first order maximum tangential stress theory of Erdogan and Sih [12] to predict the crack trajectory of an adhesively bonded narrow-body fuselage panel tested at Boeing, as shown in Figure 2. He was able to approximate the actual behavior fairly well in the gently curving region until the crack grew near to the tear strap, but was unable to predict the path as the crack turned and grew parallel to the tear strap, resulting in flapping.

The work of Kosai, Knops and others gave substantial evidence that to more accurately model crack turning behavior in pressurized cylinders, a 2^{nd} order theory was needed such as that described by Finnie and Saith [13]. (Here, 2^{nd} order refers here to the inclusion of the 2^{nd} term, or T-stress, in the asymptotic stress field in the vicinity of the crack tip, which is neglected in the Erdogan and Sih theory.) Knops was the first to implement this theory in an adaptive mesh finite element code, yet despite the improved theory his results for the Boeing narrow body panel test compare very closely with those of Potyondy. Like Potyondy, he was unable to simulate the turning of the crack in the vicinity of the stiffener, and the resulting flapping phenomena. Chen [10] also modeled the Boeing test panel using an adaptive mesh scheme and a 2^{nd} order theory that includes fracture orthotropy [14] (fracture orthotropy referring to the variation of the fracture toughness with material orientation, symmetric about two axes). His results for both isotropic and orthotropic cases are also presented in Figure 2. Note that in his isotropic run, he was for the first time able to simulate the turning of the crack at the tear strap. In the orthotropic case, he matched the first part of the trajectory considerably better, but was still unable simulate crack turning at the tear strap, because the crack was growing in the preferred direction of the 2024-T3 fuselage skin, and effect of the T-stress was insufficient to turn the crack. Despite this shortcoming, the ability to simulate crack deflection by a tear strap for the isotropic case was a significant first.

While there were various differences in the finite element implementation, it appears that the main difference in Chen's isotropic analysis which enabled him to show turning and flapping where Knops did not was the characteristic length, r_c, chosen for use in the analysis. Chen used a value of 0.09 inches which was found during finite element simulations to correlate fairly well with crack paths observed in double cantilever beam specimens reported by Pettit [4], whereas Knops used a value of 0.05 inches[1]. Attempts in the literature to evaluate r_c often give contradictory results, and the physical meaning and phenomenological basis of this parameter has not been well understood (some might question whether such a characteristic length in fact exists at all). One object of this paper is to offer a physical explanation of the existence and character of the characteristic length, and to provide an approximate means to estimate r_c from more commonly available tensile and fracture properties.

Also of importance is the accuracy of the T-stress calculation. Very recently [34], a high polynomial order (p-version) finite element code implementation of a contour integral solution for computation of the T-stress was utilized to obtain T-stress values of unprecedented accuracy. Equally as important, an error estimation parameter was developed to allow a quantitative estimate of the error associated with a given crack tip discretization geometry (referred to hereafter as the crack tip rosette). As will be shown herein, much of the error is of a systematic nature, and it is possible to calibrate a given crack tip rosette geometry against known highly accurate solutions, thus enabling correction of the error in the T-stress computation *a posteriori*..

2.0 REVIEW OF 2ND ORDER CRACK TURNING THEORY

The mixed mode expression in polar coordinates for the elastic stress field around a crack tip (Figure 3) is given by (truncating after the second term of the infinite expansion given by Williams [15])

$$\sigma_r = \frac{1}{\sqrt{2\pi r}}\cos\frac{\theta}{2}\left[K_I\left(1+\sin^2\frac{\theta}{2}\right)+\frac{3}{2}K_{II}\sin\theta-2K_{II}\tan\frac{\theta}{2}\right]+\frac{T}{2}(1+\cos 2\theta) \qquad (1)$$

$$\sigma_\theta = \frac{1}{\sqrt{2\pi r}}\cos\frac{\theta}{2}\left[K_I\cos^2\frac{\theta}{2}-\frac{3}{2}K_{II}\sin\theta\right]+\frac{T}{2}(1-\cos 2\theta) \qquad (2)$$

$$\sigma_{r\theta} = \frac{1}{2\sqrt{2\pi r}}\cos\frac{\theta}{2}\left[K_I\sin\theta+K_{II}(3\cos\theta-1)\right]-\frac{T}{2}\sin 2\theta \qquad (3)$$

Where K_I and K_{II} are the mode I and mode II stress intensity factors (Figure 4), and the T-stress is the constant, or far field stress component. A physical understanding of what the T-stress represents can be revealed by examining the radial stress of Equation (1) at $\theta=\pm\pi$, for which

[1] Actually, Knops is not explicit with regard to the value of r_c utilized for 2024-T3. However, he did quote a value for PMMA plastic plate of 1.3 mm (0.05 inches) based on the results of Ramulu and Kobayashi [Knps68,11] . Kosai, Kobayashi and Ramulu [6] later gave the same value for 2024 aluminum, and it appears that Knops used this value for both materials.

$$\sigma_r = -K_{II}\sqrt{\frac{2}{\pi r}} + T \quad at\ \theta = +\pi$$
$$\sigma_r = +K_{II}\sqrt{\frac{2}{\pi r}} + T \quad at\ \theta = -\pi \tag{4}$$

In the absence of the mode II loading, the T stress is simply the stress along the crack flank immediately behind the crack. One could imagine that the T stress could be introduced into a body with a straight crack by imposing a constant far-field stress of arbitrary magnitude parallel to the crack without affecting the stress intensity factors. However, it is intuitively apparent that if this load is sufficiently increased in tension, a propagating crack may well want to turn and grow normal to this far field stress.

While many crack turning theories have been proposed, one of the most promising is the second order maximum tangential stress theory [20,13,6], which assumes that the crack will propagate in the direction of maximum tangential stress occurring at a material specific radius, r_c, from the crack tip. To maximize σ_θ, the derivative of equation (2) is set equal to zero at $r=r_c$, which can be rearranged to obtain the transcendental equation in terms of the instantaneous turning angle, θ_c

$$\frac{K_{II}}{K_I} = \frac{-2\sin\frac{\theta_c}{2}}{(3\cos\theta_c - 1)}\left[\cos\frac{\theta_c}{2} - \frac{8}{3}\frac{T}{K_I}\sqrt{2\pi r_c}\cos\theta_c\right] \tag{5}$$

which is plotted in Figure 5 in normalized format. Note that this theory predicts turning ($\theta_c < 0$) in a pure mode I environment subject to the criterion

$$r_c > r_o = \frac{9}{128\pi}\left(\frac{K_I}{T}\right)^2 \tag{6}$$

The common first order theory [12] can be obtained either by setting $r_c=0$, or by neglecting the T-stress, which yields from Equation (5)

$$\frac{K_{II}}{K_I} = \frac{-\sin\theta_c}{(3\cos\theta_c - 1)} \tag{7}$$

This method does not require evaluation of the T stress, but as apparent from Figure 4, is expected to lose accuracy in problems where substantial positive T stresses exist (as when a crack approaches a tear strap or stiffener in a pressurized fuselage). It is further noted from the foregoing that the effect of the T-stress vanishes unless the characteristic length is non-zero.

3.0 THE CHARACTERISTIC LENGTH, r_c

3.1 Literature Review

Irwin [16], Dugdale [17] and others gave approximate expressions for the size of plastic zone in front of a crack tip in an elastic-plastic materials. Ingraffea [18] and others have shown that due to microcracking and strain softening, inelastic zones also appear about the crack tip in more brittle materials such as rock. There has been a general agreement in the literature since that the characteristic length associated crack turning should be smaller than the inelastic zones identified in these studies.

Rice and Johnson [19] discussed the role of various characteristic lengths associated with microscopic failure mechanisms in elastic plastic materials, including the crack blunting radius and void spacing, in the context of plain strain fracture problems.

The existence of the characteristic length associated with crack turning was proposed by Williams and Ewing [20], who suggested that a crack might be assumed to propagate in the direction of maximum tangential stress evaluated at a point a finite distance ahead of the crack tip. As an estimate of the characteristic length for PMMA, they referenced a previous work by Constable, Williams, and Culver [21] which identified equivalent flaw sizes based on fatigue thresholds of in polyvinyl chloride of the order of 0.0025 inches. Constable conjectured that the equivalent flaw effect might be associated with crazing.

Streit and Finnie [22] determined r_c using photoelastic methods for 7075-T651 aluminum plate to be 0.010 inches. They used the observed onset of path instability of an initially self-similar crack as the basis for determining r_c. They described r_c as the distance at which void growth or crack initiation will occur, referencing Rice and Johnson and others.

Using similar methods, Ramulu and Kobayashi [23] experimentally determined r_c for PMMA[2] to be 0.05 inches, which is quite a bit larger than had been previously expected. Theocaris and Andrianopolis [24] independently obtained similar results. Kosai and Kobayashi [25] later described r_c for PMMA as "a material constant which specifies the characteristic crack tip region in which the off-axis micro-cracks are triggered and connected to the main lead crack tip", similar to the void growth spacing assertion mentioned previously.

Kosai, Kobayashi, and Ramulu [6] later estimated r_c for 2024-T3 and 7075-T6 sheet to be 0.06 inches based on the lengths of micro-crack branches observed along dynamic fracture surfaces of test specimens. This is considerably larger than the value given by Streit and Finnie for 7075-T651 plate, but the method of determination of r_c is completely different than previous methods. Also, the reduced thickness of the sheet relative to the plate material would likely have played a role.

Pettit [4], found that path instability occurred in 2024-T3[3] DCB specimens at values of r_o at least as high as 0.11 inches due to sensitivity of the crack path to small amounts of K_{II} (as can be observed in Figure 4 near the bifurcation at $r_o=r_c$), but that the crack turning radius approached zero at $r_o = 0.05$ inches, which was subsequently used as a (likely rather poor) estimate of r_c. Because imperfections or perturbations giving rise to small amounts of K_{II} can be found in any real specimen [14], the onset of path instability in nominally symmetric specimens will always occur at an r_o value in excess of r_c, thus casting uncertainty on any r_c values obtained in that manner.

---

[2] Actually, the material used by Ramulu and Kobayashi is designated as "Homelite 100" which the author understands is a commercial form of PMMA. Also, their experiments were dynamic in nature, though they claimed that static values of r_c would be comparable.

[3] Actually, the material was of NASA vintage stock made to the earlier 24ST designation.

3.2 Present Theoretical Development

The following development will be discussed in the context of plasticity, with the focus on metallic materials. Nevertheless, the general principles described can also be applied to materials that fracture by way of micro-cracking or other inelastic effects.

A simple tensile test of a strain hardening material yields the familiar engineering and true stress-strain plots shown schematically in Figure 6 (the less familiar "Strain Softening Zone" shown at the end of the curve will be discussed later). In accordance with a well-known plastic instability theory attributed to Considere, the maximum load, F, occurs when the specimen rate of area reduction equals the rate of strain hardening [25]

$$dF = \sigma dA + A d\sigma = 0 \tag{8}$$

Rearranging,

$$\frac{d\sigma}{\sigma} = -\frac{dA}{A} = d\varepsilon$$

$$\frac{d\sigma}{d\varepsilon} = \sigma \tag{9}$$

It is equally well established that the point of maximum load also defines the onset of localized deformation or necking in the specimen. That this true can be clearly illustrated by likening the specimen to a series of nonlinear springs of unit length, as illustrated in Figure 7. Each spring may be considered to have a local spring constant $\frac{dF}{d\varepsilon}$. As the series is stretched, all the springs elongate in proportion to their compliance, $\frac{d\varepsilon}{dF}$. As the stiffness of any one of the springs becomes zero, then its compliance becomes infinite, all the other springs unload, and only that spring elongates. All along the specimen a compliance of zero is approached as the maximum load is approached, but due to some imperfection one segment reaches that point first, and necking begins there.

Once localized deformation has begun, the location of the future failure of the specimen has been determined. As fracture develops, the processes which occur after the onset of localized deformation may differ from material to material, but the location of fracture is set in a macroscopic sense at the onset of plastic instability.

Assuming strain hardening of the exponential form,

$$\sigma = k\varepsilon^m \tag{10}$$

and substituting this into equation (9), one obtains the true plastic strain at the engineering ultimate stress

$$\varepsilon_{ult} = m \tag{11}$$

Noting that $S = \sigma e^{-\varepsilon}$ (where e is the base of the natural log) we obtain from (10) and (11) the engineering ultimate stress of the material in terms of k and m

$$S_{ult} = km^m e^{-m} \tag{12}$$

Defining σ_o as the 0.2 percent offset yield strength, we have $k=\sigma_o (.002)^{-m}$ and

$$\frac{\sigma_o}{S_{ult}} = \left(\frac{.002e}{m}\right)^m \tag{13}$$

Swift [26] developed similar relationships for plastic instability and necking in sheet material under tensile plane stress conditions. Necking is also observed in front of the crack tip, and as will be shown, may play a significant role in crack path formation in sheet metal.

A crack growing in a thin sheet is illustrated in Figure 8, with the necking region shown in the vicinity of the crack tip well within the bounds of the plastic zone, since necking must occur after some plastic deformation as in the tensile test. It is further asserted based on observation that the crack will eventually develop along the necking line, and that the future crack path is therefore known out to the onset of necking (barring some abrupt change in the load environment). In order to support this notion, it is observed that the sectional load (load/in) distribution ahead of a propagating crack and normal to the future crack path (shown as σ_n in Figure 8) must have a maximum a finite distance away from the crack tip as shown schematically in Figure 9.

McMeeking [27], using nonlinear finite element computations, has shown this to be true for the self-similar plane strain stationary crack due to crack blunting. The sectional load distribution of Figure 9 is also supported by the argument that all real materials must exhibit strain softening behavior across any real failure interface down to zero load[4] as asserted in Figure 6.

It is now observed that in a manner equivalent to the Considere criterion mentioned previously, that the onset of localized deformation coincides with the instability point defined by

$$dN_n = 0 \tag{14}$$

where N_n is the sectional load normal to the future crack path. For elastic plastic strain hardening materials, this point marks the onset of plastic instability, whether in plane strain or plain stress. The path of localized deformation marks the future crack path just like

---

[4] Strain softening might alternately be described as the advanced stages of deformation localization, including void growth and coalescence for metallic materials. The interface has finite residual strength until the last two atoms of a given interface separate, (and even as they separate, they do so with a smooth load/displacement relationship). Given that the atomic bonds, even in a tensile test, must break in some sequence, and cannot separate at exactly the same moment, it follows that in the limit of absolute displacement control the failure of any interface could be defined as a quasi-static progression of damage as the load drops smoothly (at some scale) to zero. The failure interface of a slow stable tearing interface approaches this limit of absolute displacement control [18]

necking in the tensile specimen predetermines the eventual failure location. The instability point may thus be considered as the end of the known future crack path, the point where the material is "deciding" where the crack will go next. Presumably as the crack grows the instability point would migrate to the location where N_n is maximized. Thus the distance from the physical crack tip to the instability point, l_c, might be considered to physically represent the characteristic length associated with crack turning.

Unfortunately, evaluation of the generally curvilinear l_c is a daunting task. For the purposes of this study, it shall be assumed to be straight, and of approximately constant length, r_c for a given material and thickness. In order to obtain an estimate of that length, the simplest case of a self-similar crack will suffice. For the plane strain case, McMeeking and Parks [28] have already shown that the maximum stress occurs for materials with moderate strain hardening at a distance approximately given by

$$r_c \approx \frac{J}{\sigma_o} \tag{15}$$

Where for small scale yielding and mode I loading, the strain energy release rate J, is related to the stress intensity factor by

$$J = \frac{K_I^2}{E} \tag{16}$$

Thus for plain strain we may write

$$r_c \approx \frac{K_I^2}{\sigma_o E} \tag{17}$$

It should be cautioned, however, that while this expression is a reasonable estimate for plain strain with T=0, it has been shown [40] that the distance to the maximum stress point varies with the T-stress, particularly if it is negative.

For the plane stress case, thickness strain (necking) is possible. We can thus rewrite (14) as

$$dN_n = dN_\theta = t d\sigma_\theta + \sigma_\theta dt = 0 \tag{18}$$

$$\frac{d\sigma_\theta}{\sigma_\theta} = -\frac{dt}{t} = -d\varepsilon_z \tag{19}$$

Assuming incompressibility,

$$-d\varepsilon_z = d\varepsilon_\theta(1+\rho) \tag{20}$$

where $\rho = \frac{\varepsilon_r}{\varepsilon_\theta}$

Using the Von Mises yield condition, the differential equivalent strain can be expressed as

$$d\bar{\varepsilon} = d\varepsilon_\theta \frac{2}{\sqrt{3}}\left(1+\rho+\rho^2\right) \tag{21}$$

Combining (19), (20), and (21) and noting that for a constant ρ, the equivalent stress conforms to the equality $\frac{d\bar{\sigma}}{\bar{\sigma}} = \frac{d\sigma_\theta}{\sigma_\theta}$ we obtain

$$\frac{d\bar{\sigma}}{d\bar{\varepsilon}} = \frac{\bar{\sigma}\sqrt{3}(1+\rho)}{2\left(1+\rho+\rho^2\right)} \tag{22}$$

Assuming an exponential strain hardening relationship for the equivalent stress and strain similar to (10), we obtain the critical strain and stress at the instability point.

$$\bar{\varepsilon}_{crit} = \frac{2m\left(1+\rho+\rho^2\right)}{\sqrt{3}(1+\rho)} \tag{23}$$

$$\bar{\sigma}_{crit} = k\left[\frac{2m\left(1+\rho+\rho^2\right)}{\sqrt{3}(1+\rho)}\right]^m \tag{24}$$

Assuming the necking region in plane stress is somewhat larger than the crack blunting effected zone in plane strain (which will be observed hereafter), we can obtain an estimate of ρ based on the Hutchinson Rice Rosengren (HRR) asymptotic field for plane stress cracks in strain hardening materials [29,30, 31]. This inherently involves the assumption of proportional flow, which for a propagating crack is less than desirable. Directly ahead of a straight propagating crack, the flow should be fairly proportional, but the deviation from proportionality will have an unknown effect on the results forward of the crack. Also of concern is the fact that the HRR field is derived based on the assumption of small strain theory. The very existence of plastic instability is by definition a large strain effect. Nevertheless, McMeeking and Parks did observe in their analysis that the plane strain HRR field was valid up to the point of maximum stress. Note also that true stress and strain and engineering stress and strain are fairly close up until plastic instability for most structural materials. Proceeding with the above cautions in mind, the effective stress given by the HRR solution, written here in terms of the far field stress intensity factor, is

$$\bar{\sigma} = \sigma_o\left[\frac{K_I^2}{\alpha\sigma_o^2 I_n r}\right]^{\frac{1}{n+1}} \sigma_e(n,\theta) \tag{25}$$

For $\theta = 0$, Hutchinson normalized the σ_e term to unity for the plane stress case. The Ramberg-Osgood material parameters α and n are related to the exponential strain hardening parameters from Equation (10) by

$$k = \sigma_o^{(1-1/n)}\left(\frac{E}{\alpha}\right)^{1/n} \tag{26}$$

$$m = 1/n \tag{27}$$

Hutchinson gives numerical results for I_n and ρ which are functions of the exponent n. For the propagating crack, we may assume that K_I is equal to the propagating value, which for stable tearing may be denoted K_c. We may thus approximately equate (24) and (25) at $r=r_c$, and to obtain after some rearrangement

$$r_c \approx \left(\frac{\sqrt{3}}{2} \frac{\sigma_o \alpha n (1+\rho)}{E(1+\rho+\rho^2)} \right)^{\frac{(n+1)}{n}} \left[\frac{K_c^2}{\alpha \sigma_o^2 I_n} \right] \tag{28}$$

Equation (28) can be combined with equations (12), (26), and (27) to obtain an expression in terms of the engineering ultimate strength

$$r_c \approx \left(\frac{\sqrt{3}}{2} \frac{(1+\rho)}{(1+\rho+\rho^2)} \right)^{(1+1/n)} \frac{n}{I_n e^{1/n}} \left[\frac{K_c^2}{S_{ult} E} \right] \tag{29}$$

For n<7, ρ makes little contribution, and I_n is nearly linear at least up to the maximum value of n=13 given by Hutchinson, and probably well beyond. Thus, in this range we can further approximate with no significant loss of accuracy

$$r_c \approx \left(\frac{\sqrt{3}}{2} \right)^{(1+1/n)} \left(\frac{n}{(3.38 - .039n) e^{1/n}} \right) \left[\frac{K_c^2}{S_{ult} E} \right] \tag{30}$$

If a suitable value for n is not available, one can obtain an approximation using the ratio of yield and ultimate strength from the implicit equation

$$\frac{\sigma_o}{S_{ult}} = (.002 n e)^{1/n} \tag{31}$$

which was obtained by combining equations (13) and (27).

A predicted r_c value for 2024-T3 alloy is given in Table 1 based on Equations (30) and (31). The mechanical properties are B basis values from MIL-HDBK-5G [32], and the fracture toughness the maximum R-curve value obtained based on 48 inch wide R-curve panels reported by Gruber et al [33]. The predicted r_c value is in satisfactory agreement with the value chosen by Chen to match observed crack paths. One caution, however, is that the value of Kc used is only reached after 4-5 inches of stable tearing, whereas the coupon test data achieved crack turning after less than an inch of growth, at which point the characteristic length associated with necking should have been considerably smaller.

Table 1. Calculation of r_c for 2024-T3

.063 inch, 2024-T3 clad							r_c
	S_y (ksi)	S_{ult} (ksi)	n	K_c (ksi$\sqrt{in}$)	E (ksi)	$K_c^2/S_{ult}E$	Plane Stress
LT	42	62	8.04	180	10500	0.050	0.098

4.0 CALCULATION OF ACCURATE T-STRESS VALUES

4.1 Literature Review

T-stress calculations have been performed by various authors. Larsson and Carlsson [35] evaluated the T-stress using finite elements. Leevers and Radon [36] directly imposed the infinite series solution given by Williams [15] in a variational approach to obtain estimates of K_I and T simultaneously. They gave estimates of the T-stress in the form of the dimensionless parameter B, where

$$B = \frac{T\sqrt{a}}{K_I} \tag{32}$$

Based on the convergence observed, Leevers and Radon estimated the error in the B values provided to be less than three percent. Sham [37] used 2nd order weight functions and a work conjugate integral to calculate T-stresses in various specimen configurations. Fett [38, 39] introduced a Green's function approach to calculate T-stresses, and analyzed numerous configurations. A more approximate displacement correlation method was outlined by Al-Ani and Hancock [40] which is nevertheless easy to implement in plate and shell codes, and has been utilized in various forms by other authors [4, 9, 10].

Cardew et al [41] and Kfouri [42] computed the T-stress using a modified J-integral based on unpublished work of Eshelby, and also gave results for selected specimens based on finite element analyses. Another type of path independent integral based on the Betti-Rayleigh reciprocal theorem has also been proposed [43,44], and shown to be mathematically equivalent to the J-integral method by Chen et al [34]. By implementing the contour integral solution into a high polynomial order (p-version) finite element program, Chen obtained T-stresses that were claimed to be numerically exact to six significant figures. The numerical accuracy was verified by way of an exact benchmark solution (a crack tip and surrounding region with the exact boundary conditions applied corresponding to arbitrary combinations of K_I, K_{II}, and T) and a theoretical error relationship

$$e_T = T_{FE} - T = \tilde{e}_T \frac{K_I}{\sqrt{r_1}} \tag{33}$$

where e_T is the error in the computed T-stress, r_1 is the characteristic dimension of the integration zone (typically taken as external radius for circular zones, half side length for square zones), and $\tilde{e}_T$ represents the discretization error in the vicinity of the integration zone.

4.2 Error Correction

Equation (33) was derived by recognizing that the stress contribution of the singular terms in the stress field will converge far slower than the contribution of the non-singular terms, leaving an error in the coefficients of all terms proportional to the coefficients of the

singular terms[5]. The square root term in the denominator was included due to dimensional considerations, consistent with the form of Equations (1-3). Based on the convergence rate argument, terms of higher order than T are expected to contribute little error, though this was not checked in the benchmark example, since higher order terms were excluded.

Note that unlike the error estimation expression given in [34], Equation (33) is given with no absolute value signs to enforce that the error measure always be positive. As shown in Figure 10 for the integration path and rosette geometry of Chen, $\tilde{e}_T$ is virtually constant and characteristically negative[6] for a element polynomial order, p, above 12. The error is thus systematic, and can thus be corrected as shown in the next section. The relative error of the T-stress can be expressed in a manner consistent with the characteristic sign of the error.

$$e_{T_{rel}} = \frac{e_T}{|T|} = \tilde{e}_T \frac{K_I}{|T|\sqrt{r_1}} \tag{34}$$

The assertion that the relative error scales with $K_I/T\sqrt{r_1}$ is supported by the fact that geometrically similar finite element models that differ only by a scaling factor (which also implies that the integration zone is likewise scaled) will have the same relative error. Considering the rosette as a finite element model with imposed boundary conditions representing K_I and T, and recognizing the similarity of all K_I and T fields relative to a characteristic length $(K_I/T)^2$, one may therefore conclude that the combination of such a field with a rosette model of fixed geometry and scale relative to the field characteristic length will be similar (and thus have comparable relative error) to all other rosette/field combinations with the same relative scaling ratio.

Because $\tilde{e}_T$ represents the discretization error in the vicinity of the integration zone, it should thus be relatively constant so long as the mesh geometry, or rosette, within the integration zone is geometrically similar for all problems. The mesh geometry outside of the integration zone is of secondary influence, and may change from problem to problem, thus its effect will be treated as a probabilistic source of error. Nevertheless, provided that the external mesh is reasonably proportioned, the error introduced should be relatively small.

Not noted in the previous paper is the fact that the err or in K_I likewise scales to itself,

$$e_{K_I} = K_{IFE} - K_I = \tilde{e}_{K_I} K_I \tag{35}$$

No characteristic length is necessary because all K fields are similar without respect to a characteristic length. Thus, the relative error in K_I is approximately constant for a given integration path/rosette geometry

---

[5] K_{II} was also found to pollute T slightly, but at a level orders of magnitude lower than K_I. It would thus likely have even a lesser effect on K_I, thus it is hereafter neglected. In nearly pure mode II loading, however, the effect of K_{II} might be significant, and could be normalized in a similar manner.

[6] Note that the characteristic sign consistency of the error may not hold if the crack tip elements are included in the integration zone, as will be explained. Also the sign of the error may change with p.

$$e_{K_I\,rel} = \frac{e_{K_I}}{K_I} = \tilde{e}_{K_I} \tag{36}$$

As shown in Figure 11, e_{KI} is constant and characteristically positive for the integration path/crack tip rosette geometry of Chen p>9, after which the benefit of increasing p is lost for this rosette geometry, and error of the opposite sign appears to take over. A similar correction is surely possible for K_{II}, but is not discussed at present.

If the sign of the error is always the same, Equations (33) and (36) can be utilized to correct the finite element solutions for K_I and T. Designating T_{adj} and K_{Iadj} as the adjusted values

$$T \approx T_{adj} = T_{FE} - \tilde{e}_T \frac{K_I}{\sqrt{r_1}} \tag{37}$$

$$\begin{aligned} K_I \approx K_{Iadj} &= K_{IFE} - \tilde{e}_{K_I} K_I \\ &\approx K_{IFE} \Big/ \left(1 + \tilde{e}_{K_I}\right) \end{aligned} \tag{38}$$

The adjusted values so obtained will still vary from the exact, because in practice $\tilde{e}_T$ and $\tilde{e}_{K_I}$ are distribution functions, and can be characterized with mean values and standard deviations. As mentioned previously, the random component of the error may be associated with mesh variations outside the rosette and solution oscillation at the crack tip. In fact, if the equivalent domain integrals for K_I and T are evaluated including in the domain the crack tip elements themselves, the random component of error may be larger than the systematic error, resulting in overall errors which may vary in sign, and are thus less correctable. For this reason it is recommended that the crack tip elements be excluded from the integration zone.

In order to evaluate Equations (37) and (38), one must have an estimate of the calibration factors $\tilde{e}_T$ and $\tilde{e}_{K_I}$. For individual cases with known exact or highly accurate reference solutions, sample values of $\tilde{e}_T$ and $\tilde{e}_{K_I}$ can be obtained as

$$\tilde{e}_T = \left(T_{FE} - T\right) \Big/ \frac{K_I}{\sqrt{r_1}} \tag{39}$$

$$\tilde{e}_{K_I} = e_{K_I} = T_{FE} - T \tag{40}$$

The mean and standard deviation can estimated based on models of a sampling of reference solutions, preferably over a range of stress intensity factors and integration radii. For the data in Figures 10 and 11, three samples of each error parameter were evaluated at each polynomial order p. Average values of the correction factors are given in Table 2 given to eight computed places, which are likely all significant for p=1, but perhaps only one digit is significant at p=12.

Table 2. Average Values of the Correction Factors

p	$\tilde{e}_{K_I}$	$\tilde{e}_T$
1	4.7282230E-01	-1.8830976E-01
2	1.0063271E-01	-2.7370718E-02
3	2.1770302E-02	-5.8434480E-03
4	4.5650887E-03	-6.7037228E-04
5	9.1459033E-04	-1.9170107E-04
6	1.7818900E-04	-5.0844804E-05
7	3.2591667E-05	-7.4061435E-06
8	4.3786667E-06	-2.3991630E-06
9	-3.1936667E-07	-4.2137896E-07
10	-9.3926667E-07	-9.3609849E-08
11	-8.1720000E-07	-2.1412723E-08
12	-6.4710000E-07	2.5544523E-09

Using these values, the solutions were corrected resulting in the miniscule errors in T_{adj} and KI_{adj} indicated by the error bands in Figures 10 and 11. Note that the error obtained in this manner is independent of p. Nevertheless, this example is not realistic because the models were completely similar—not just similar in the vicinity of the integration zone.

In order to obtain a more realistic representation, K_I and T estimates from the DCB specimen geometry presented in [34] was adjusted according to Equations (37) and (38) to obtain the data given in Figure 12. Each analysis used the same six-tiered rosette used in the benchmark example, with the integration zone encompassing the first layer of elements outside the crack tip elements as before, thus the correction factors given in Table 2 were applicable. As expected, the benefit of correction in this real case is nearly as good as for the benchmark solution. Nevertheless, the improvement in the accuracy of KI is typically an order of magnitude or more, though not as good as at low p values. The improvement in T due to correction is about half an order of magnitude.

The rosette geometry utilized, however, is very poor at low p values, which are common in available finite element codes. FRANC2D, a two-dimensional fracture code developed at Cornell University, utilizes a more suitable crack tip rosette made up of eight six-node quarter-point singular elements as shown in Figure 14. FRANC2D is being used as a platform to develop crack turning analyses, thus it is of interest to calibrate the rosette for T-stress calculations. Due to the use of singular elements, the accuracy of stress intensity factors calculated by FRANC2D is typically within one percent, thus no correction is necessary there.

Figure 14 shows a rosette subdivided once with the inner radius equal to one-half the outer radius. The standard version of FRANC2D allows the user to manipulate the number of subdivisions and the subdivision ratio. A subdivision ratio of 0.5 was selected for this study. Also, the version of FRANC2D utilized has been updated to include the contour integral solution for T. It was also found that FRANC2D models cracks with a small initial crack opening, which causes numerical difficulties when evaluating the contour integrals. As a temporary solution, gap elements with zero interference were specified to close the crack prior to running the analyses.

In order to provide data from which to evaluate $\tilde{e}$, several runs were made, analyzing selected specimens for which highly accurate reference solutions were obtained by Chen et al. The error in the computed T-stresses is shown in normalized fashion in Figure 15. For this rosette geometry/integration path of Figure 14, it was found that

$$\tilde{e}_T = -0.00825 \pm .00255$$

(Mean) (Std. Deviation)

A plot of the corrected data with lines denoting various confidence levels is given in Figure 15. The average error (50% confidence level) of the corrected solution was about on fifth of the original error.

5.0 CONCLUSION

The characteristic length associated with crack turning, r_c, has been characterized as the distance ahead of the crack tip at which plastic instability occurs for both plane strain and plane stress fracture problems in strain hardening materials. An estimated plane stress r_c value has been determined for 2024-T3, and compares favorably with a recent value given in the literature which results in good correlation with test data. Nevertheless, due to the many severe assumptions associated with the plane stress solution caution is recommended with regard to its use pending further evaluation.

An error correction methodology has been developed for the T-stress, which can also be applied to stress intensity factors. With this methodology, the accuracy of a contour integral based T-stress algorithm has been substantially increased, and an estimate of the remaining error is provided.

6.0 REFERENCES

1. J. Maclin, "Performance of Fuselage Pressure Structure", *1991 International Conference on Aging Aircraft and Structural Airworthiness*, Washington D.C., November 19-21, 1991, NASA Conference Pub 3160 (1992).

2. T. Swift, "Damage Tolerance in Pressurized Fuselage", 11th Plantema Memorial Lecture, 14th Symposium of the ICAF, New Materials and Fatigue Resistant Aircraft, Ottawa, Canada, June 1987 (also Douglas Paper 7768).

3. T. Swift, "Application of Damage Tolerance Technology to Type Certification", SAE Paper #811062, Aerospace Congress and Exposition, Anaheim, CA October 1981.

4. R. G. Pettit, J. C. Newman, M. S. Domack, *Crack Turning Damage Tolerance Approach for Integrally Stiffened Structure*, 19th ICAF Symposium, International Committee on Aeronautical Fatigue, Edinburgh, June 1997.

5. *National Transportation Safety Board Aircraft Accident Report, Aloha Airlines Flight 243, Boeing 737-200, N73711, Near Maui, Hawaii, April 28, 1988*, NTSB/AAR-89/03, 1989.

6. M. Kosai, A. S. Kobayashi, M. Ramulu, "Tear Straps in Aircraft Fuselage", *Durability of Metal Aircraft Structures*: Proc. of International Workshop on Structural Integrity of Aging Airplanes, Atlanta Technology Publications, Atlanta, GA, pp. 443-457, 1992.

7. M. Miller, K. Kaelber, and R. E. Worden, "Finite Element Analysis of Pressure Vessel Panels", *Durability of Metal Aircraft Structures*: Proc. of International Workshop on Structural Integrity of Aging Airplanes, Atlanta Technology Publications, Atlanta, GA, pp. 337-339, 1992.

8. D. O. Potyondy, P. A. Wawrzynek, A. R. Ingraffea, "Discrete Crack Growth Analysis Methodology for Through Cracks in Pressurized Fuselage Structures", *International Journal of Numerical Methods in Engineering*, Vol. 38, No 10., pp.1611-1633.

9. B. Knops, *Numerical Simulation of Crack Growth in Pressurized Fuselages*, Ph.D. Thesis, Delft University of Technology, September, 1994.

10. C. Chen, Ph.D. Thesis, Department of Civil and Environmental Engineering, Cornell University, 1998.

11. P. A. Wawrzynek, A. R. Ingraffea, "Interactive Finite-Element Analysis of Fracture Processes: An Integrated Approach", *Theoretical and Applied Fracture Mechanics*, Vol. 8, 1987, pp. 137-150.

12. F. Erdogan, G. C. Sih; "On the Extension of Plates under Plane Loading and Transverse Shear", *Journal of Basic Engineering*, Vol. 85D, No. 4, pp. 519-527, 1963.

13. I. Finnie, A. Saith; "A Note on the Angled Crack Problem and the Directional Stability of Cracks", *International Journal of Fracture* , Vol.9, pp.484-486,1973.

14. R. G. Pettit, J. J. Wang, C. Toh, *Integral Airframe Structures (IAS)—Validated Feasibility Study of Integrally Stiffened Metallic Fuselage Panels for Reducing Manufacturing Cost*, Boeing Report CRAD-9306-TR-4542, NASA contract NAS1-20014, Task 34, November, 1998.

15. M. L. Williams, "On the Stress Distribution at the Base of a Stationary Crack", ASME Transactions, *Journal of Applied Mechanics*, Vol. 24, 1957.

16. G. R. Irwin, "Plastic Zone Near a Crack and Fracture Toughness", *Proc. 7th Sagamore Conf.*, p. IV-63, 1960.

17. D.S. Dugdale, "Yielding of Steel Sheets Containing Slits", *Journal of the Mechanics and Physics of Solids*, Vol. 8, pp. 100-108, 1960.

18. A. R. Ingraffea, "Theory of Crack Initiation and Propagation in Rock", *Fracture Mechanics of Rock*, Academic Press/Harcourt Brace Jonavich, pp.71-110, 1987.

19. J. R. Rice, M. A. Johnson, "The Role of Large Crack Tip Geometry Changes in Plane Strain Fracture", *Inelastic Behavior of Solids*, McGraw Hill, pp. 641-690, 1969.

20. J. G. Williams, P. D. Ewing, "Fracture Under Complex Stress—The Angled Crack Problem", *International Journal of Fracture Mechanics*, Vol. 8, No. 4, December 1972.

21. I. Constable, J. G. Williams, L.E. Culver, "Notch Root Radii Effects in the Fatigue of Polymers", *International Journal of Fracture Mechanics*, Vol. 6, No. 3, pp. 279-285, 1970.

22. R. Streit, I. Finnie, "An Experimental Investigation of Crack-Path Directional Stability", *Experimental Mechanics*, Vol. 20, pp. 17-23, 1980.

23. M. Ramulu, A. S. Kobayashi, "Dynamic Crack Curving—A Photoelastic Evaluation", *Experimental Mechanics*, Vol. 23, pp.1-9, 1983.

24. P. S. Theocaris, N. P. Andrianopoulos, N. P., "A Modified Strain Energy Density Criterion Applied to Crack Propagation", *Journal of Applied Mechanics*, Vol. 49, No. 1, pp. 81-86, 1982.

25. W. S. Hosford, R. M Caddell, *Metal Forming—Mechanics and Metallurgy, Prentice Hall*, p. 69, 1993.

26. H. W. Swift, "Plastic Instability Under Plane Stress", *Journal of the Mechanics and Physics of Solids*, Vol. 1, pp. 1-18, 1952.

27. R. M. Mc Meeking, "Finite Deformation Analysis of Crack-Tip Opening in Elastic-Plastic Materials and Implications for Fracture", *Journal of the Mechanics and Physics of Solids*, Vol. 25, pp. 357-381, 1977.

28. R. M. McMeeking, D. M. Parks, "On Criteria for J-Dominance of Crack Tip Fields in Large-Scale Yielding", ASTM STP 668, American Society for Testing and Materials, Philadelphia, pp. 175-194, 1979.

29. J. W. Hutchinson, "Singular Behaviour at the End of a Tensile Crack in a Hardening Material", *Journal of the Mechanics and Physics of Solids*, Vol. 16, pp. 13-31, 1968.

30. J. R. Rice, G. F. Rosengren, "Plane Strain Deformation Near a Crack Tip in a Power-Law Hardening Material", *Journal of the Mechanics and Physics of Solids*, Vol. 16, pp. 1-12, 1968.

31. J. W. Hutchinson, "Plastic Stress and Strain Fields at a Crack Tip", *Journal of the Mechanics and Physics of Solids*, Vol. 16, pp. 337-347, 1968.

32. MIL-HDBK-5G, *Metallic Materials and Elements for Aerospace Vehicle Structures*, Vol. 1, pp. 3-73, November, 1994.

33. M. L. Gruber, C. J. Mazur, K. E. Wilkins, R. E. Worden, *Investigation of Fuselage Structure Subject to Widespread Fatigue Damage*, Federal Aviation Administration Report DTFA03-94-C-00065,pp. 12-13, October 1995.

34. C. Chen. R. Krause, R. Pettit, A. Ingraffea, "Numerical Assessment of T-stress Computation Using a p-version Finite Element Method", Cornell Fracture Group publication in progress, December, 1998.

35. S. G. Larsson, A. J. Carlsson, "Influence of Non-Singular Stress Terms and Specimen Geometry on Small-Scale Yielding at Crack Tips in Elastic-Plastic Materials, *Journal of the Mechanics and Physics of Solids*, Vol. 21, pp. 263-277, 1973.

36. P. S. Leevers, J. C. Radon, "Inherent Stress Biaxiality in Various Fracture Specimen Geometries", *International Journal of Fracture*, Vol. 19, pp.311-325, 1982.

37. Sham, T.-L. Sham, "The Determinationof the Elastic T-term Using Higher Order Weight Functions", *International Journal of Fracture*, Vol. 48, pp. 81-102, 1991.

38. T. Fett, "A Green's Function for T-stresses in an edge-cracked rectangular plate, *Engineering Fracture Mechanics*, Vol. 57, pp. 365-373, 1997

39. T. Fett, *A Compendium of T-stress Solutions*, Institut fur Materialforschung, Karlsruhe, Report FZKA 6057, February 1998.

40. A. M. Al-Ani and J.W. Hancock, "J-Dominance of Short Cracks in Tension and Bending", *Journal of the Mechanics and Physics of Solids,* Vol. 39, No.1, pp. 23-43, 1991.

41. G. E. Cardew, M. R. Goldthorpe, I. C. Howard, A. P. Kfouri, "On the Elastic T-term", *Fundamentals of Deformation and Fracture: Eshelby Memorial Symposium*, 1985.

42. A. P. Kfouri, "Some Evaluations of the Elastic T-term using Eshelby's Method", *International Journal of Fracture*, Vol. 30, pp. 301-315, 1986.

43. J. Sladek, E. B. Becker, R. S. Durham, "A Contour Integral Computation of Mixed-Mode Stress Intensity Factors", International Journal of Fracture, Vol. 12, pp. 359-368, 1976.

44. F. G. Yuan, S. Yang, "The Application of Fracture Mechanics to Stitched Warp-kit Fabric Composites", AIAA Paper #98-2025, *39th AIAA/ASME/ASCE/AHS/ASC Structures, Structural Dynamics, and Materials Conference*, Long Beach, CA, April 1998.

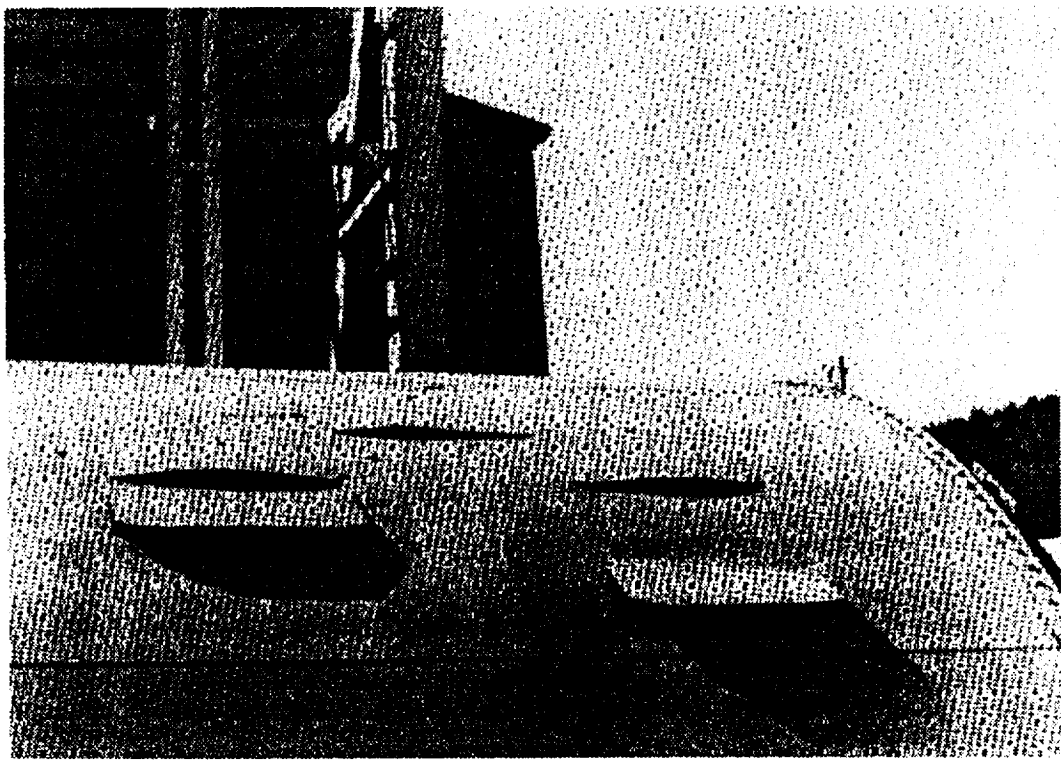

Figure 1. Crack Turning and Flapping in Boeing 707 Test Panel [1]

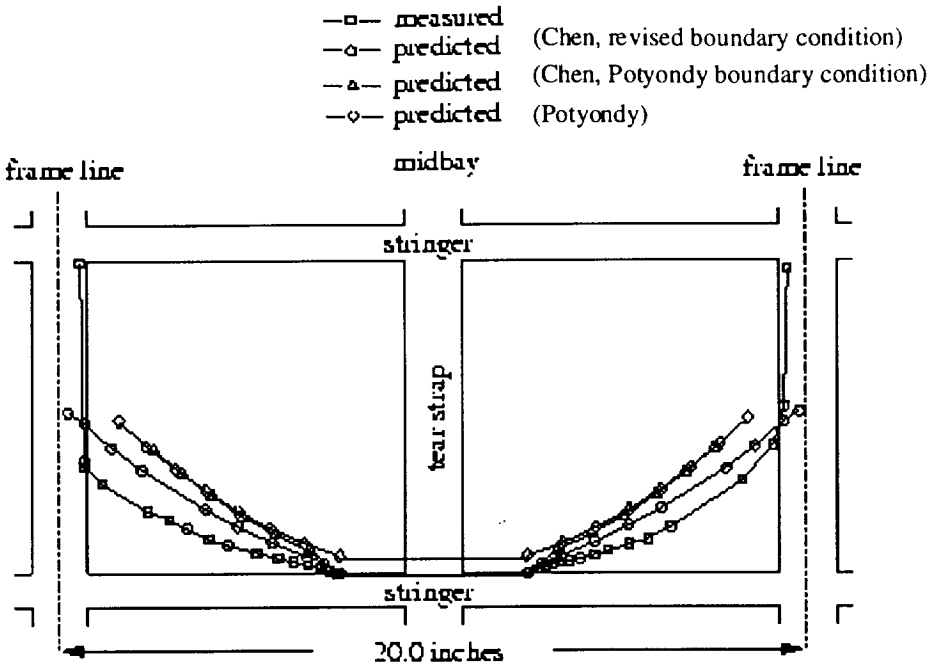

a.) first order maximum tangential stress theory

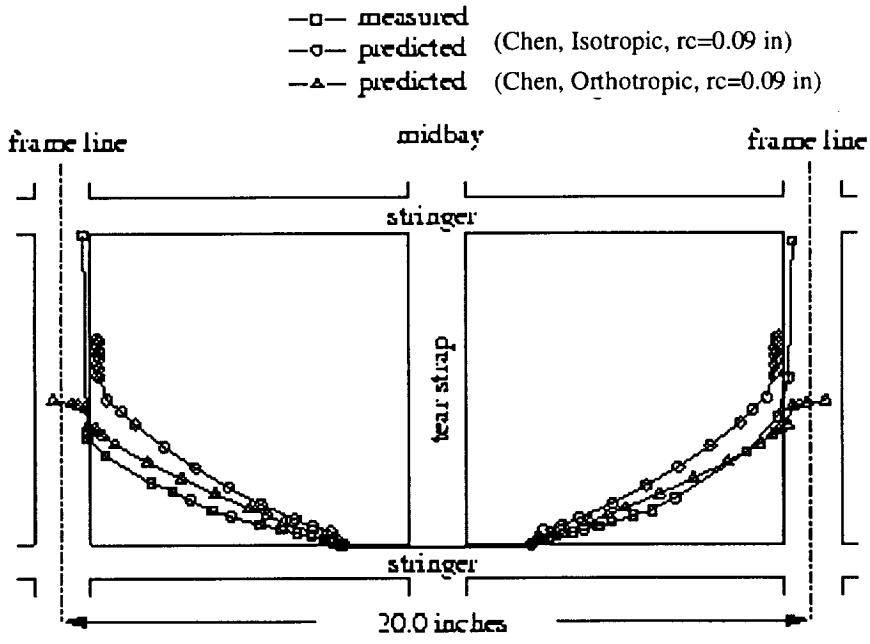

b) Second order maximum tangential stress theory

Figure 2. Correlation of Crack Growth Simulations of Various Investigators (from [10])

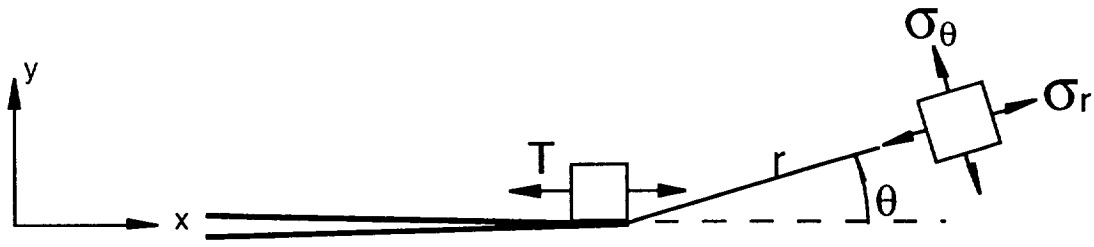

Figure 3. Polar Coordinate System About a Crack Tip, also Showing Physical Meaning of the T-Stress

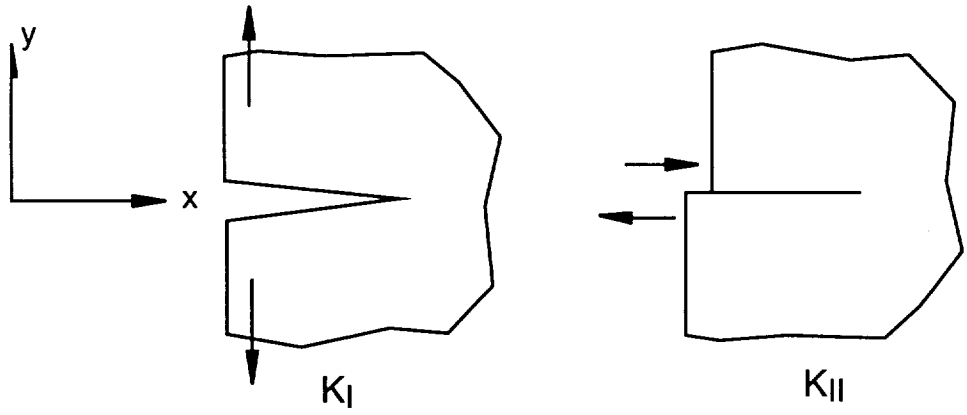

Figure 4. Mode I and Mode II Loading of a Cracked Body (Shown with Positive Sign)

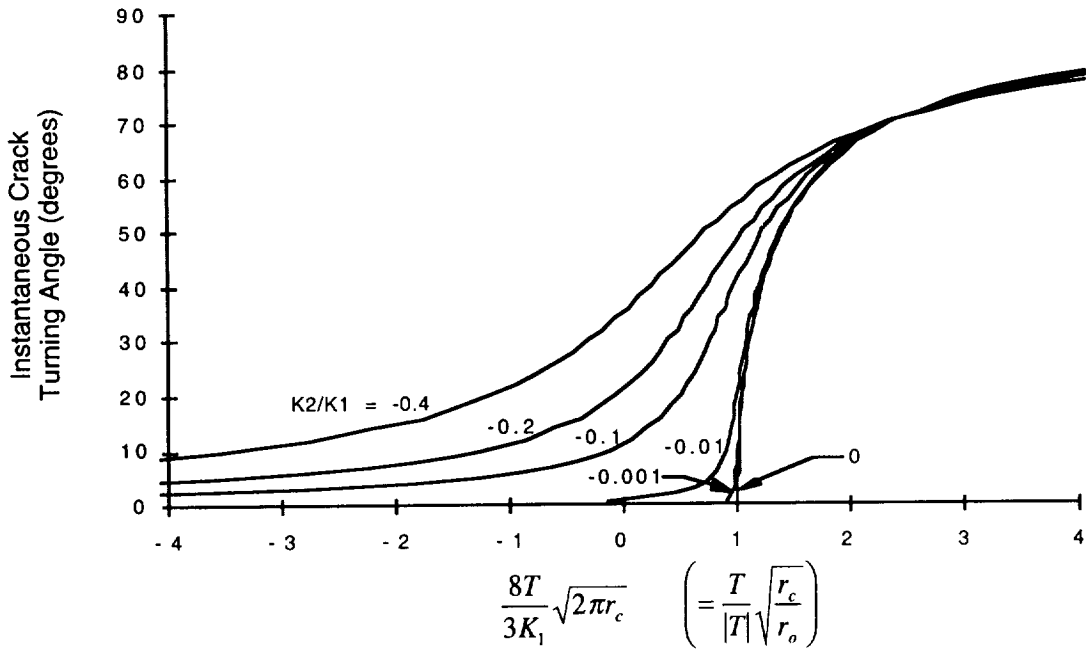

Figure 5. Instantaneous Crack Turning Angle as a Function of Normalized Field Parameters

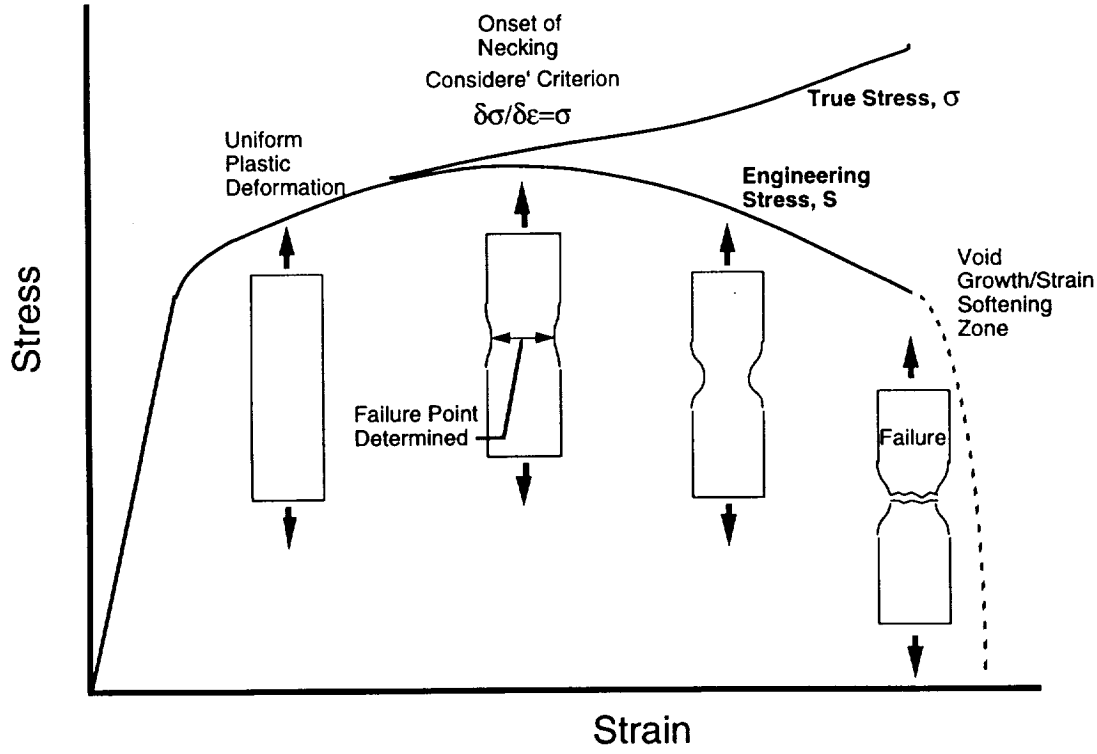

Figure 6. Schematic of Typical Tensile Test of Strain Hardening Material

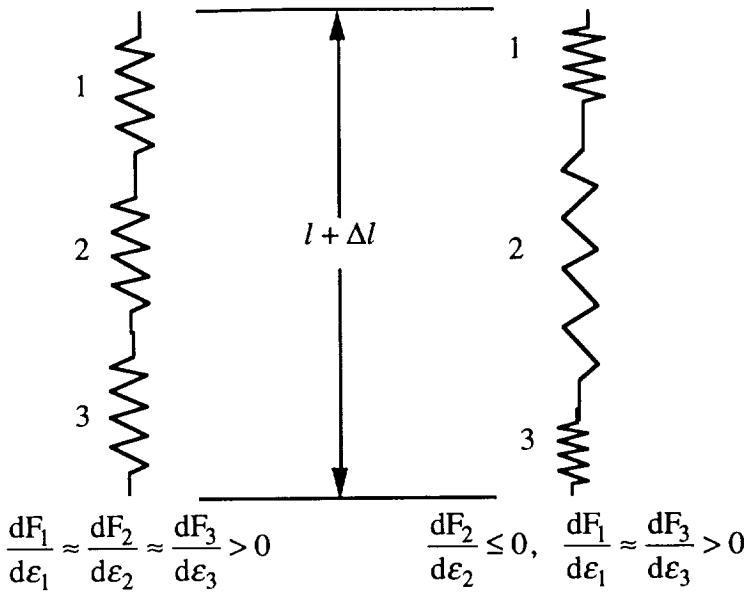

Figure 7. Illustration of Instability Principle Using Nonlinear Springs

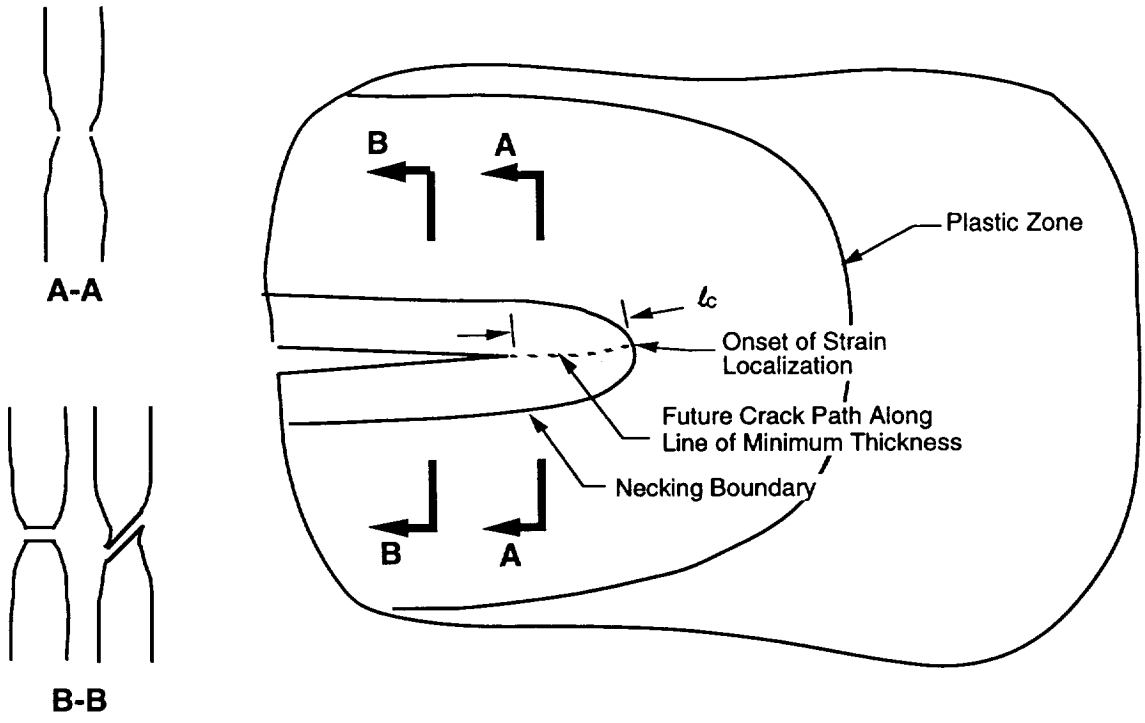

Figure 8. Schematic Physical Process Zones in the Vicinity of a Propagating Crack

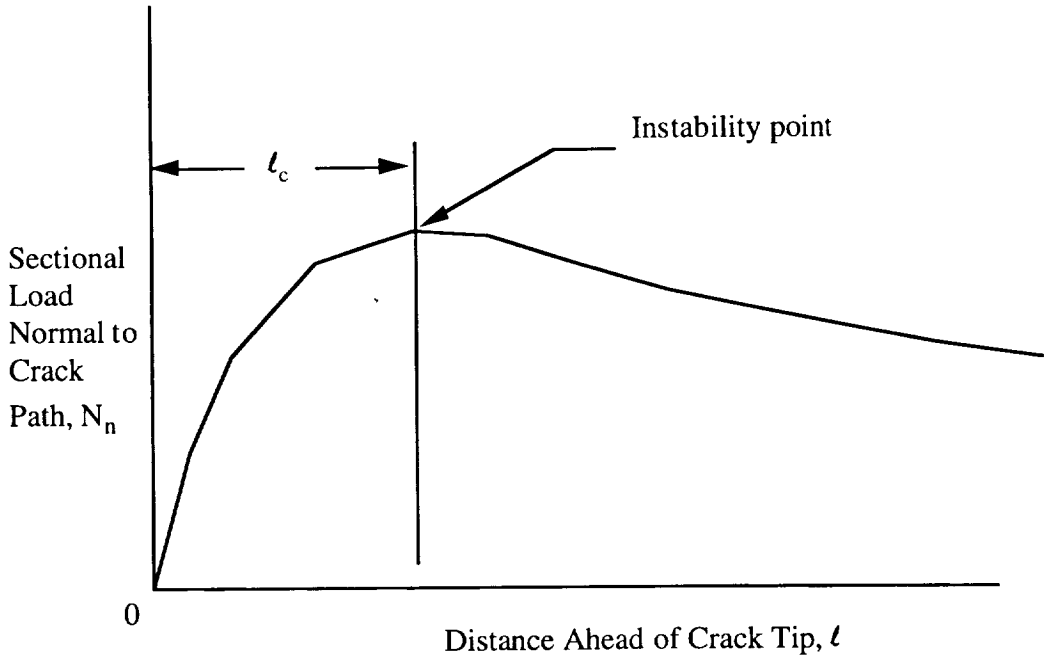

Figure 9. Schematic of Sectional Load Distribution ahead of Crack Tip

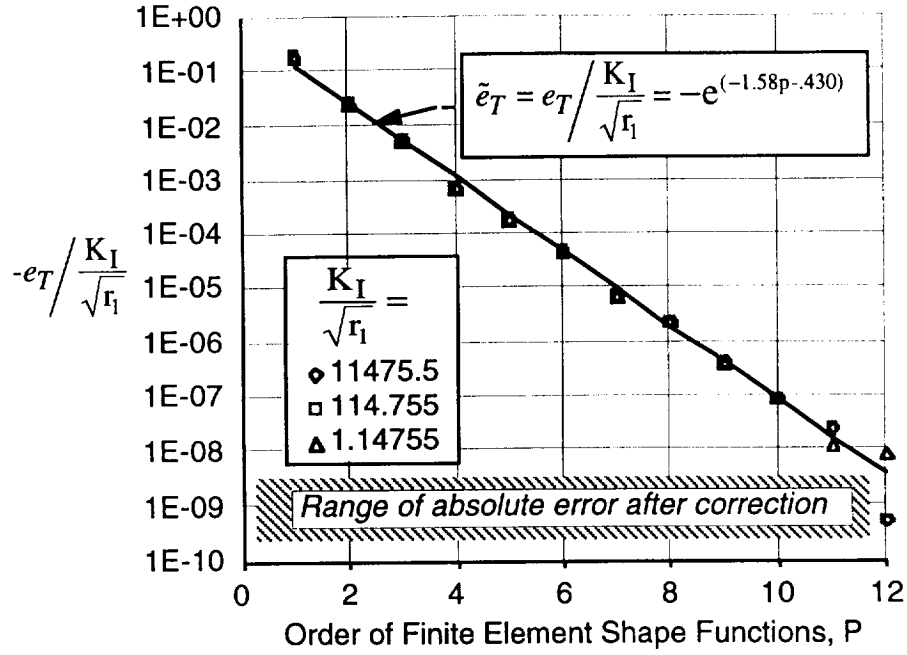

Figure 10. Accuracy Assessment of T Computations Using p-version Contour Integral Implementation of Chen et al [34]

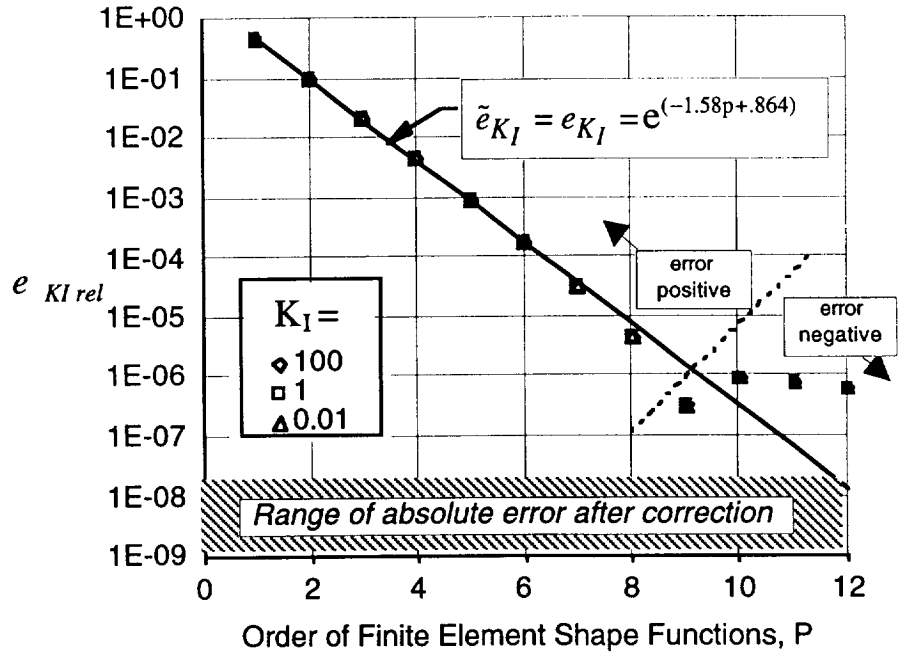

Figure 11. Accuracy Assessment of K_I Computations Using p-version J-Integral Implementation of Chen et al[34]

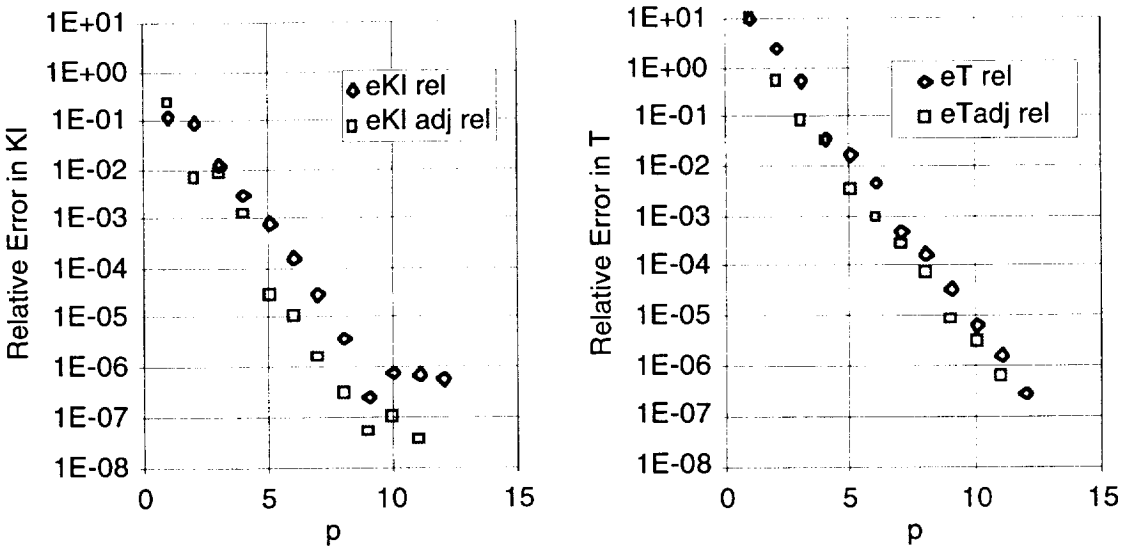

Figure 12. Comparison of Error in as-Calculated and Corrected Values of K_I and T in a Double Cantilever Beam Specimen, h/w=.2, a/w=.5

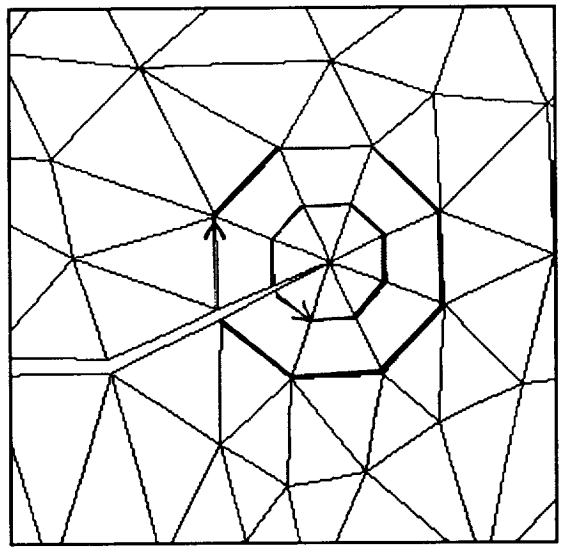

Figure 13. Geometry and Integration Path Used for FRANC2D Rosette Calibration

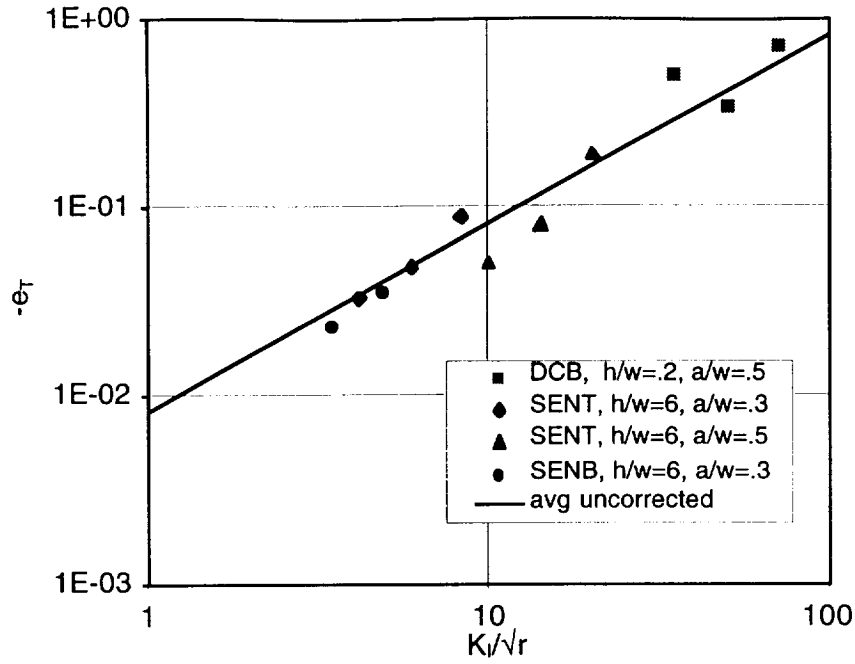

Figure 14. As-Calculated Error in T-stress Using FRANC2D

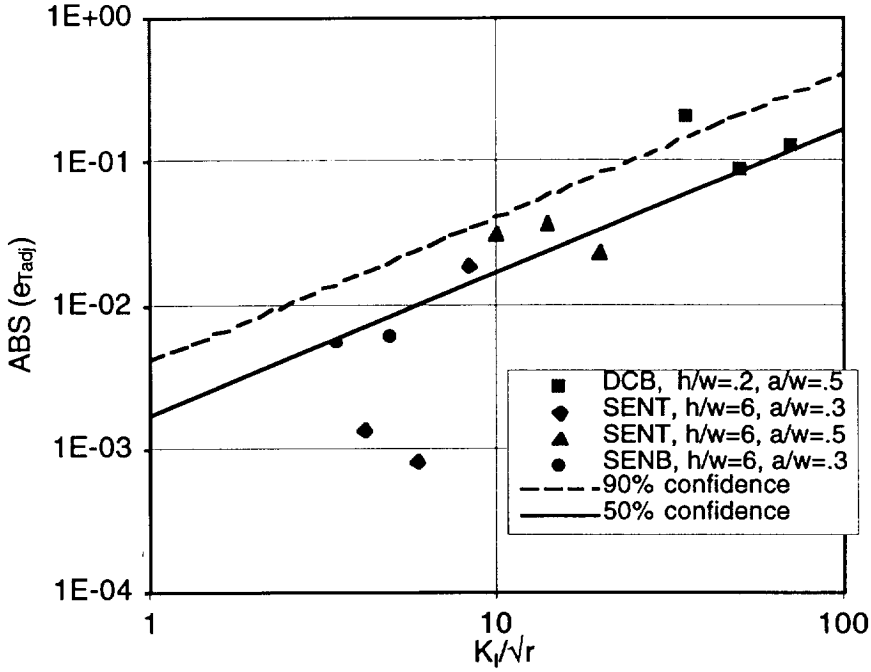

Figure 14. Corrected Error in T-stress Calculated by FRANC2D with Upper Bounds Representing Estimated Error

An Evaluation of Crack Tip Opening Criteria for Crack Propagation and Turning

Richard G. Pettit
Anthony R. Ingraffea

Cornell Fracture Group

Attachment #2 to Final Report
NASA Contract NAG-1-2013

December, 1999

An Evaluation of Crack Tip Opening Criteria for Crack Propagation and Turning

Richard G. Pettit Chuin-Shan Chen Anthony R. Ingraffea

Cornell Fracture Group

Abstract

Elastic-plastic Crack Tip Opening Displacement (CTOD) criteria proposed for crack propagation and turning [1,2,3] are examined in the context of linear elastic fracture mechanics. In particular, the use of the CTOD as a crack turning criterion is discussed as an extension of the mode I dominant criterion of Cotterel and Rice [4] by simulating plastic deformation via a virtual crack kink which opens in pure mode I or pure mode II. The mode I dominant case is found to result in a crack turning theory similar to the second order maximum tangential stress theory with a transition to mode II deformation anticipated under certain conditions.

INTRODUCTION

Crack turning has been studied by many investigators [5], and is well recognized as a potentially important phenomenon in structural applications, such as crack turning and flapping in aircraft fuselage structures [6, 7]. Crack path prediction using linear elastic maximum tangential stress theory [8, 9] has been most commonly used in structural analysis. For crack turning and flapping phenomena and other problems, the effect of the second order, or T-stress term in the asymptotic stress field has been shown to be very important [10, 11]. Approximate theories have accounted for the directional variation of fracture properties in anisotropic materials [12, 13]. Inclusion of the T-stress term in the linear elastic theory requires the use of a material dependent characteristic length parameter, r_c, associated with the process zone size. Because the process zone presumably sizes with the plastic zone, it follows that the effect of the T stress will increase with the extent of the plastic zone. This observation has been used to explain quantitatively why slow fatigue crack growth turns more gradually than static tearing of thin aluminum sheets [11] .

As computational hardware and software have become increasingly powerful, nonlinear finite element analysis of complex structures has become more viable, leading to an increased emphasis on elastic-plastic methods to predict crack propagation and trajectory in situations where the effects of plasticity are potentially significant. To date these efforts have focussed on isotropic materials. Early work in this field showed that plasticity can effect the crack trajectory [14], and supported a notion that crack propagation and trajectory could be correlated with critical CTOD values [1, 2]. Sutton et al [3] recently proposed curves based on results from a small scale yielding (SSY) boundary layer crack tip model and laboratory experiments which can be used to infer the crack growth direction from the ratio of the mode I and mode II CTOD components. The curves include a transition from mode I to mode II dominated crack extension that has been observed by previous investigators [2, 15], and were used to predict stable tearing crack paths in various specimens, with very encouraging results.

The CTOD crack trajectory curves appeared to be independent of the T-stress [3], and yet seemed to adequately capture the small turning radius of statically tearing cracks in a high T stress environment. Thus, questions were raised about the influence of the T-stress on crack trajectory, and how or if its effect is captured by the CTOD approach. In an attempt to address these issues, the CTOD method is examined from a surrogate linear elastic standpoint, once again including the effects of plasticity and the T-stress by virtue of a characteristic length.

2ND ORDER LINEAR ELASTIC SURROGATE FOR ELASTIC-PLASTIC THEORY

Consider a lead crack under plane stress conditions with a plastic zone as shown in Figure 1a. Compared to an elastic crack, the plastic zone results in additional deformation that can be approximated by a virtual elastic crack kink as shown in Figure 1b. For self-similar crack growth, Wells [15], used the Irwin plastic zone correction as an approximation of the effective elastic kink length to obtain an estimate of the CTOD. While the appropriate choice of length may remain in question, it is not unreasonable to assert that for a given material and loading, there is a unique kink length, b_c, and orientation, θ_c, which will best simulate the deformation field as one moves away from the crack tip into the elastic region[1]. It is further postulated that a crack kink so defined would provide a reasonable approximation of the future crack trajectory. For a crack propagating under steady-state conditions, b_c would be expected to assume a constant, material-dependent value.

As the case of perfect elasticity is approached (as for so-called brittle materials, and also approximately for slow fatigue crack growth), the length of the virtual kink necessarily vanishes. In this limiting case, Cotterel and Rice [4] concluded that the crack propagates in pure mode I, which is equivalent to the criterion $K_{II}=0$. For the finite virtual kink, it is not clear that this will continue to be the case, and based on the experimental observations [2, 15], depending on the loading conditions, cracks are observed to develop trajectories corresponding either to pure mode I or pure mode II crack opening. For the time being, it will be assumed that the virtual kink tip will operate at pure mode I, but the possibility of pure mode II propagation will also be considered.

Isida and Nishino [17] give a solutions for a crack in an infinite plate with a kink at one end which can be superimposed to obtain results for general K_I, K_{II}, and T loading. The stress intensity factors at the kink tip, k_I, and k_{II}, may be expressed as

$$\begin{aligned} k_I &= F_I^{(1)}K_I + F_I^{(3)}K_{II} - F_I^{(2)}T\sqrt{\pi a} \\ k_{II} &= F_{II}^{(1)}K_I + F_{II}^{(3)}K_{II} - F_{II}^{(2)}T\sqrt{\pi a} \end{aligned} \qquad (1)$$

Where a is the crack length, and $F_n^{(i)}$ are functions of the kink angle, θ, and the normalized kink length, b/a. The crack length parameter can be eliminated by normalizing in the form

[1] It is suggested for future study that the virtual crack kink dimensions be selected to give an equivalent J integral (evaluated at a radius somewhat large compared to the kink length) to the elastic-plastic crack.

$$\frac{k_I}{K_I} = F_I^{(1)} + F_I^{(3)}\frac{K_{II}}{K_I} - \frac{F_I^{(2)}}{\sqrt{b/a}}\frac{3}{8\sqrt{2}}\overline{T}$$
$$\frac{k_{II}}{K_I} = F_{II}^{(1)} + F_{II}^{(3)}\frac{K_{II}}{K_I} - \frac{F_{II}^{(2)}}{\sqrt{b/a}}\frac{3}{8\sqrt{2}}\overline{T} \qquad (2)$$

where $\sqrt{b/a}$ factors cleanly out of functions $F_n^{(2)}$, and $\overline{T}$ is defined with $b=b_c$ in a manner similar to that utilized for the maximum stress theory [11pettit97].

$$\overline{T} = \frac{8}{3}\frac{T}{K_I}\sqrt{2\pi b_c} \qquad (3)$$

Values of the crack propagation angle, θ_c, can be obtained by varying θ to enforce $K_{II} = 0$ for various combinations of K_{II}/K_I, and $\overline{T}$, as presented in Figure 2a. Also shown for comparison is the 2nd order maximum tangential stress theory in normalized format [9, 7, 11] with its characteristic length, r_c. Note that the two theories are nearly equivalent (though not identical) if one recognizes that the characteristic lengths differ at the bifurcation by a constant factor,

$$b_c = 2.21 r_c \qquad (4)$$

Considering that the 2nd order maximumum tangential stress theory is well regarded for its ability to predict physically observed phenoma, this similarity is encouraging. For the ideal linear elastic case, b_c=0, and the crack turning criterion becomes a function of K_{II}/K_I independent of the T-stress. This is plotted in Figure 3 in terms of the crack tip opening displacements using the notation of Sutton [3]

$$\alpha = \arctan\left(\frac{D_{II}}{D_I}\right) \qquad (5)$$

Where D_I and D_{II} are the mode I and mode II components of crack opening, with the observation that for the linear elastic case, $D_{II}/D_I = K_{II}/K_I$.

For the kinked-crack representation of the elastic-plastic crack tip, the crack tip opening displacements may be approximated as indicated in Figures 4a and 4b, depending on whether the virtual crack is assumed to develop in pure mode I or pure mode II. Assuming the CTOD is measured in a finite element simulation some small distance, d, behind the physical crack tip (the physical crack being represented by the base of the kink), the following relations may be obtained.

$$\frac{D_{II}}{D_I} = \frac{-\sin\theta_c}{\cos\theta_c + d/b_c} \qquad \text{for a pure mode I kink} \qquad (6a)$$

$$\approx -\tan\theta_c \qquad (\text{approximation for } d/b_c \rightarrow 0) \qquad (6b)$$

$$\frac{D_{II}}{D_I} = \cot\theta_c \qquad \text{for a pure mode II kink} \qquad (7)$$

Clearly these equations are approximate, but are most accurate and meaningful for small d/b_c. As d/b_c becomes large, D_{II}/D_I must approach the elastic K_{II}/K_I of the physical crack tip, and the effect of plasticity and the T-stress on the turning angle is lost. In the limit as $d/b_c \rightarrow 0$, the Equations (6,7) simply state that for mode I dominant growth, the crack grows perpendicular to the CTOD, and for mode II dominant growth, the crack grows parallel to the CTOD. Based on the linear elastic infinitesimal kink theory, no combination K_I and K_{II} at the tip of the unkinked crack results in a pure mode I kink at an angle above 74.45 degrees. The theory predicts this limiting value only when the lead crack is loaded in pure mode II (the corresponding value predicted by the maximum tangential stress theory is 70.5 degrees). With a finite (virtual) kink length, the limiting value becomes a slight function of the T-stress, but only at very long kinks or very high T-stresses. If, as postulated for isotropic materials, the virtual kink must be pure mode I or pure mode II, then one might expect that the crack would transiton to a non-mode I failure at kink angles approaching 74.45 degrees. Sutton observed a trasition to mode II failure at kink angles of about 70 degrees in 2024-T3 aluminum, under partially mode I loading conditions. Note however, there appears to be no transition whatsoever in materials such as plexiglass, which under pure mode II loading have been observed to kink consistently at angles very near the maximum stress theory value of 70.5 degrees [18].

Sutton [3] reported 2-D simulations[2] using an elastic/small-deformation plasticity model of a edge crack in a 30.4 inch radius circular plate of 2024-T3 aluminum. The crack tip was centered on the model, and traction boundary conditions were applied representing various amounts of K_I, K_{II} and T. For a given loading, the CTOD components D_I and D_{II} were first measured at a distance d=0.04 inches behind the crack tip, after which the crack was extended 0.0076 inches as a physical kink in several trial directions to find the kink angle, θ_c that resulted in the maximum total CTOD a small distance back from the kink tip. The total CTOD in this case is given by

$$CTOD_{kink} = \sqrt{\delta_I^2 + \delta_{II}^2} \tag{8}$$

where δ_I and δ_{II} are the CTOD components near the kink tip. Sutton found that the kink orientation that produced the maximum CTOD also produced nearly pure mode I or mode II displacement near the kink tip, which further supports the foregoing assumptions with regard to the mode mixity of the virtual kink.

With the plane stress plastic zone for 2024 on the order of inches, it is expected that d/b_c for Sutton's model is sufficiently small to allow the tangent approximation of Equation (6b). Equations (6b) and (7) are compared with test data and CTOD-based crack turning angle data Figure 3, showing good correllation for both mode I and mode II cases.

DISCUSSION

Note that the development of Equations (6) and (7) makes no assumption with regard to the T-stress, or even K_I or K_{II}. The primary assumption is that the opening of the virtual kink will be either pure mode I or pure mode II. Inasmuch as Figure 2a is also based on pure

[2] Several of the details given here were not included in the referenced paper, but were provided via private correspondence with Dr. Sutton.

mode I opening of the virtual kink tip, it is clear that several different combinations of K_I, K_{II}, and T acting about the physical crack tip can result in the same kink angle. Thus, it appears that D_{II}/D_I measured near an elastic-plastic crack tip will be fairly uniquely related to θ_c, but will not be uniquely related to K_{II}/K_I if plasticity is significant, and the T-stress is substantially non-zero.

Also worth mentioning is the likelihood that even as the crack tip nears a stiffener or other geometric feature, the virtual kink might still open in pure mode I or mode II. While the plastic zone shape would be distorted by the presence of such irregularities (which would likely affect the crack turning angle), the assumptions associated with the derivation of equations (6) and (7) are still valid with sufficiently small d, and the crack trajectory should remain a substantially unique function of D_{II}/D_I.

It is significant to observe that the driving features of the crack turning phenomenon appear to be adequately represented by a small deformation theory finite-element method used by Sutton. In particular, such a method neglects near-tip strain localization such as necking or crack tip blunting, and void growth and coalescence. It thus appears that the length scale associated with crack trajectory is larger than the length scales associated with these near-tip phenomena.

REFERENCES

1. J. C. Newman, D. S. Dawicke, M. A. Sutton, and C. A. Bigelow, "A Fracture Criterion for Widespread Cracking in Thin Sheet Aluminum Alloy", *17th Symposium of the International Committee on Aeronautical Fatigue(ICAF 93)*, Stockholm, 1993.

2. B. E. Amstutz, M. A. Sutton, D. S. Dawicke, and J. C. Newman, "An Experimental Study of CTOD for Mode I/Mode II Stable Crack Growth in Thin 2024-T3 Aluminum Specimens," *Fracture Mechanics,* Vol. 26, ASTM STP 1256, 1995.

3. M. A. Sutton, X. Deng, F. Ma, J. C. Newman, "A Mixed-Mode I/II Fracture Criterion and its Application in Crack Growth Predictions", (publication pending), 1998.

4. B. Cotterel, J. R. Rice, "Slightly Curved or Kinked Cracks", International Journal of Fracture, vol. 16, pp. 155-169, 1980.

5. K. Zaal, A Survey of Crack Path Stability Criteria and Their Application to Crack Flapping Phenomena in Stiffened Structures, Report LR-681, TU Delft, Faculty of Aerospace Engineering, The Netherlands, September, 1992.

6. J. Maclin, "Performance of Fuselage Pressure Structure", *1991 International Conference on Aging Aircraft and Structural Airworthiness*, Washington D.C., November 19-21, 1991, NASA Conference Pub 3160 (1992).

7. M. Kosai, A. S. Kobayashi, M. Ramulu, "Tear Straps in Aircraft Fuselage", *Durability of Metal Aircraft Structures*: Proc. of International Workshop on Structural Integrity of Aging Airplanes, Atlanta Technology Publications, Atlanta, GA, pp. 443-457, 1992.

8. F. Erdogan, G. C. Sih; "On the Extension of Plates under Plane Loading and Transverse Shear", *Journal of Basic Engineering*, Vol. 85D, No. 4, pp. 519-527, 1963.

9. I. Finnie, A. Saith; "A Note on the Angled Crack Problem and the Directional Stability of Cracks", *International Journal of Fracture* , Vol.9, pp.484-486,1973.

10. B. Knops, *Numerical Simulation of Crack Growth in Pressurized Fuselages*, Ph.D. Thesis, Delft University of Technology, September, 1994.

11. R. G. Pettit, J. C. Newman, M. S. Domack, *Crack Turning Damage Tolerance Approach for Integrally Stiffened Structure*, 19th ICAF Symposium, International Committee on Aeronautical Fatigue, Edinburgh, June 1997.

12. T. J. Boone, P. A. Wawrzynek, and A. R. Ingraffea, Engineering Fracture Mech., Vol. 26, No. 2, pp. 185-201, 1987.

13. R. G. Pettit, J. J. Wang, C. Toh, *Integral Airframe Structures (IAS)—Validated Feasibility Study of Integrally Stiffened Metallic Fuselage Panels for Reducing Manufacturing Cost*, Boeing Report CRAD-9306-TR-4542, NASA contract NAS1-20014, Task 34, November, 1998.

14. C. F. Shih, "Small-Scale Yielding Analysis of Mixed Mode Plane-Strain Crack Problems", *Fracture Analysis*, ASTM STP 560, pp. 187-210, 1984.

15. N. Hallback, F. Nilsson, "Mixed-Mode I/II Fracture Behaviour of an Aluminum Alloy", J. Mech. Phys. Solids, Vol. 42, No. 9, pp. 1345-1374, 1994.

16. A. A. Wells, "Unstable Crack Propagation in Metals: Cleaveage and Fast Fracture", *Proceedings of the Crack Propagation Symposium*, Vol. 1, Paper 84, Cranfield, UK, 1961.

17. M. Isida, T. Nishino, "Formulae of Stress Intensity Factors at the Tips of Kinked Cracks Under Various Loadings", *Engineering Fracture Mechanics*, Vol. 36, No. 5 , pp. 697-711, 1990.

18. Vaughn, H. "Crack Propagation and the Principal-Tensile Stress Condition for Mixed-Mode Loading", *Engineering Fracture Mechanics*, Vole 59, pp. 393-397, 1998.

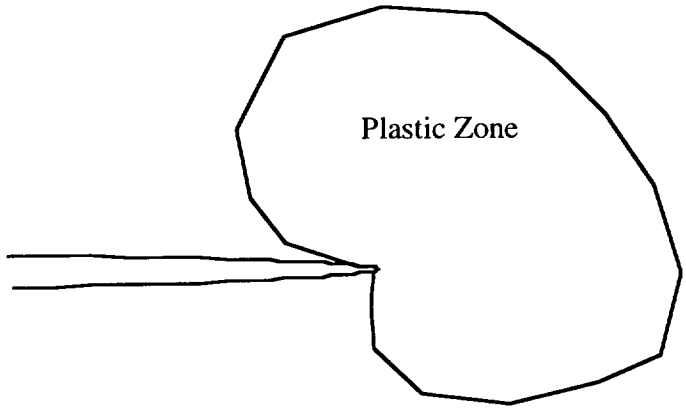

a) Physical crack tip and plastic zone

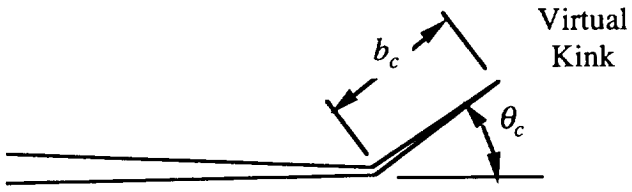

b) Physical crack with virtual kink

Figure 1. Crack Tip Plastic Zone Deformation Simulated by an Effective Virtual Kink

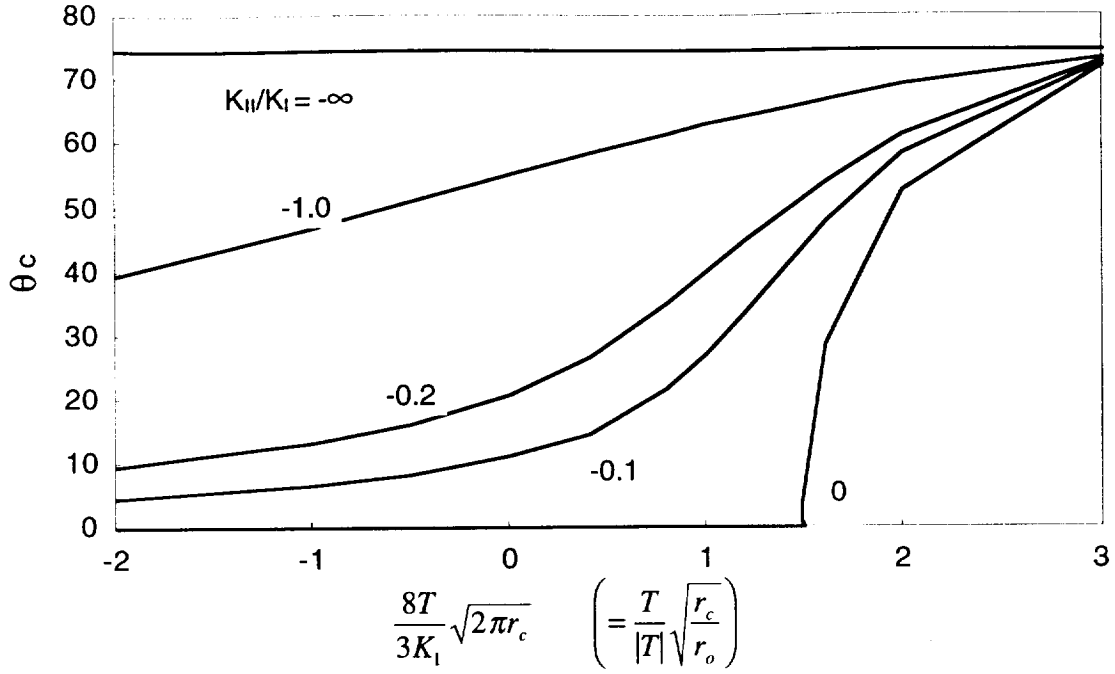

a) Virtual kinked crack with pure mode I opening (K_{II}=0)

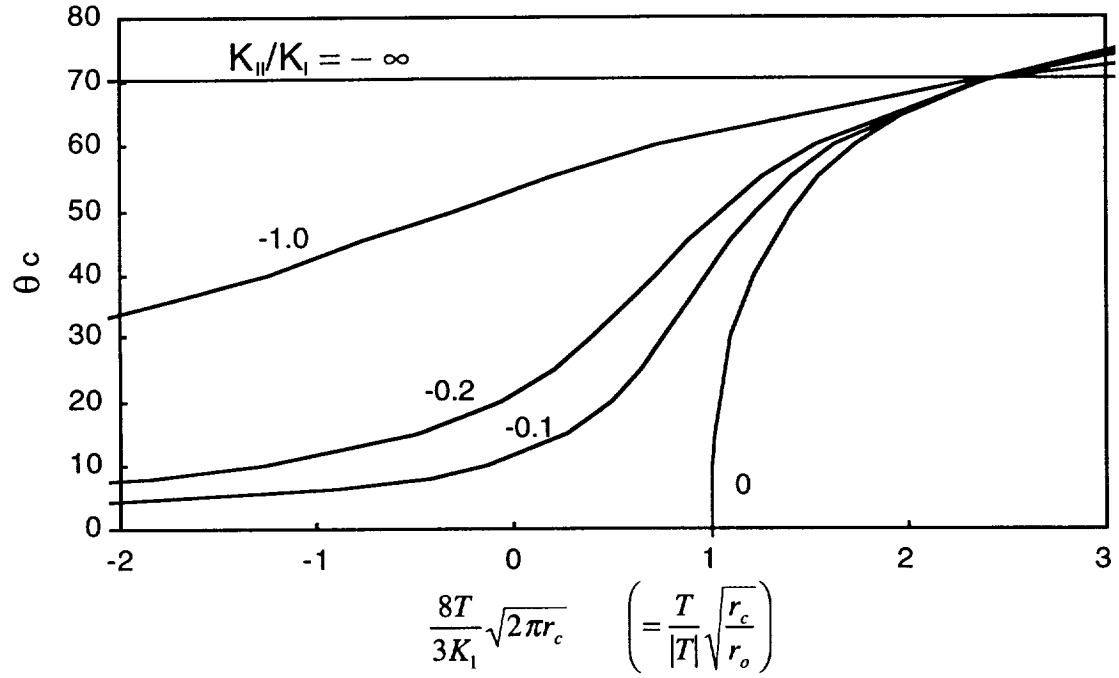

b) 2nd order maximum tangential stress theory

Figure 2. Comparison of Mode I Virtual Kink Theory with Maximum Tangential Stress Theory

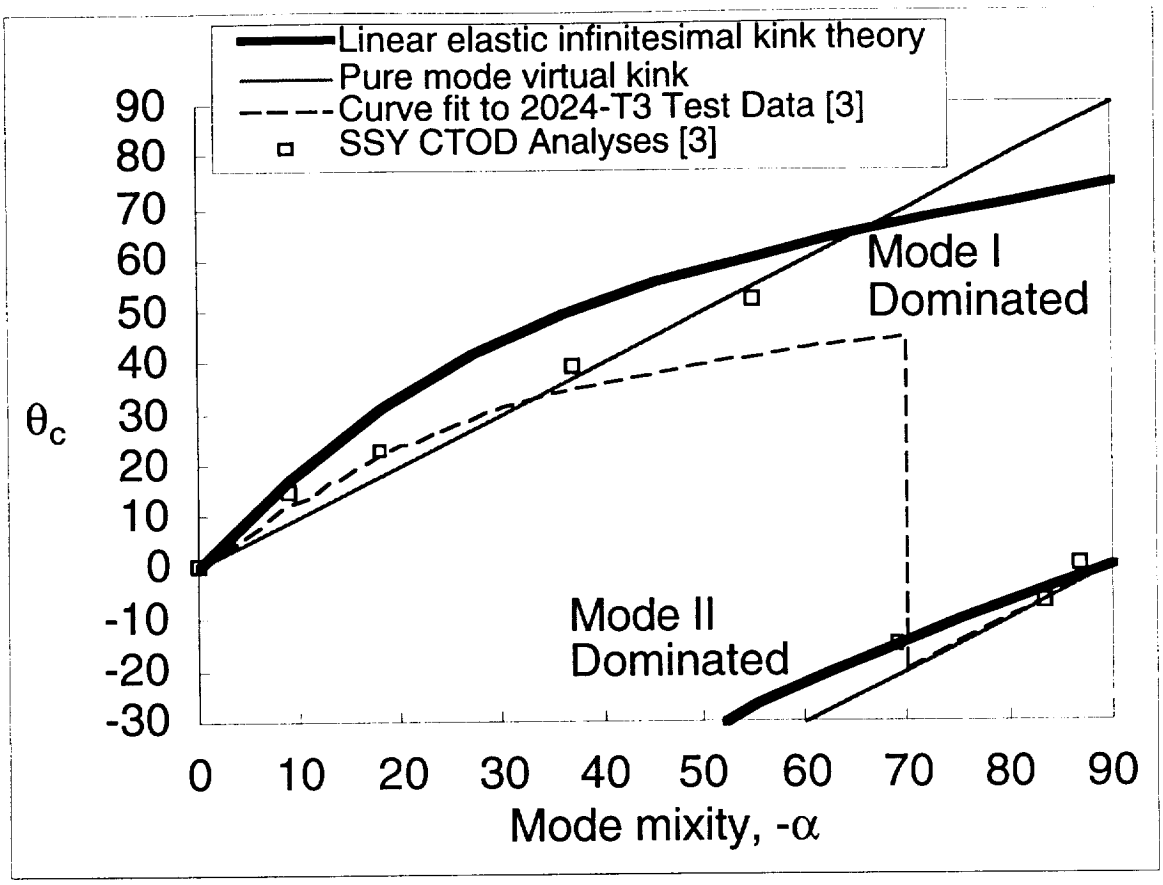

Figure 3. Comparison of Various CTOD related Crack-Turning Curves, including the data of Sutton [3]

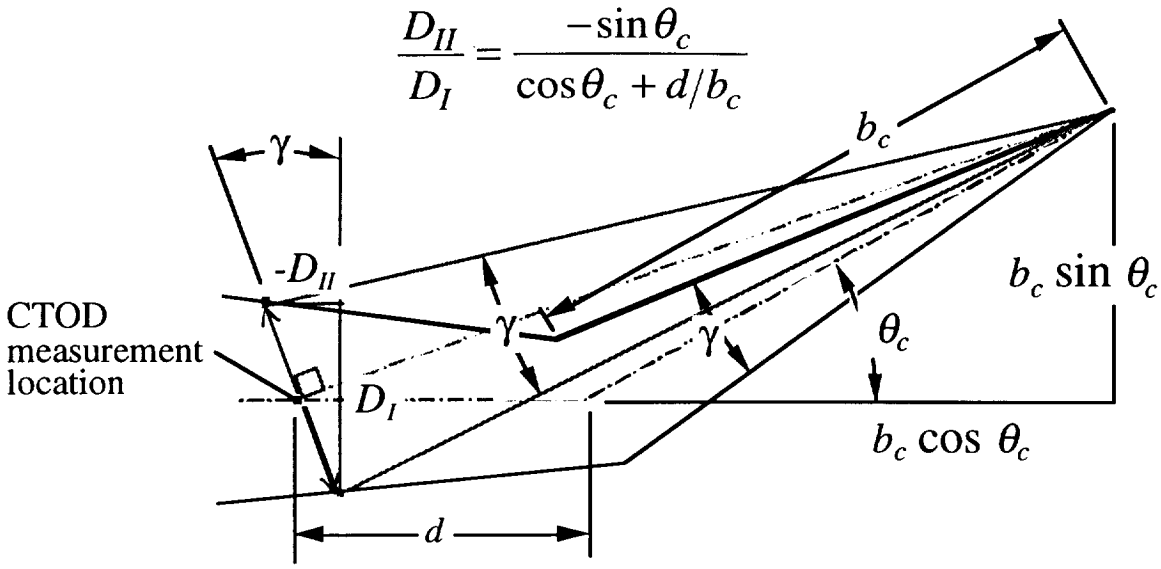

a). Pure Mode I

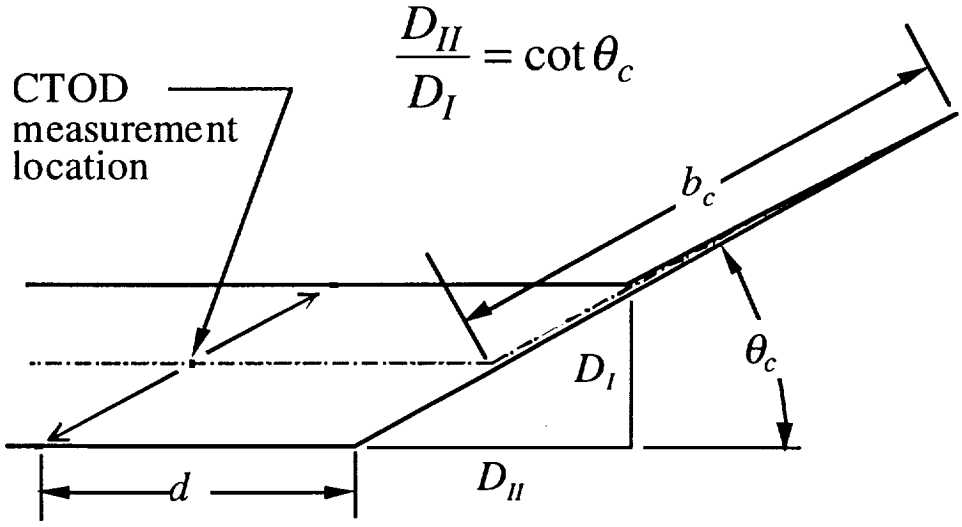

b) Pure Mode II

Figure 4. Approximate Method of Obtaining CTOD Mode Mixity for Pure Mode I and Mode II Virtual Crack Kinks